Rivista Italiana di Paleontologia e Stratigrafia	volume 120	no. 2	5 pls.	pp. 191-214	July 2014

FIRST EVIDENCE FOR LATE NORIAN PROGRADATION OF JULIAN PLATFORM TOWARDS SLOVENIAN BASIN, EASTERN SOUTHERN ALPS

LUKA GALE [1], BOŠTJAN ROŽIČ [2], EVA MENCIN [2] & TEA KOLAR-JURKOVŠEK [1]

Received: March 17, 2014; accepted: May 27, 2014

Key words: upper Triassic, stratigraphy, microfacies analysis, Slatnik Formation, Dachstein Limestone, platform evolution.

Abstract. The late Triassic in the Southern Alps is marked by an extensive growth of carbonate platforms. Whereas Dolomia Principale dominates the western and central sections, Dachstein Limestone dominates the eastern side of the Southern Alps on the so-called Julian Platform in what is now NW Slovenia. Younger tectonic movements greatly deformed the original configuration of the Julian Platform and its margins are consequently poorly preserved. While late Tuvalian and early Norian platform progradation has been recorded on the northern and eastern side of the platform, no such information is available for the southern edge of the platform, where it borders the deeper Slovenian Basin. Three detailed sedimentological sections from the southern slopes of the Jelovica plateau span from the top of the basinal Bača dolomite to the Slatnik Formation and the prograding slope of the Dachstein Limestone. The progradation has been dated as late Norian in age, and can be correlated to a poorly-expressed coarsening event recorded in previously known sections of the Slovenian Basin. In contrast to deeper parts of the basin, shallow water conditions were established on the Jelovica plateau by the beginning of the Rhaetian.

Introduction

The Norian and Rhaetian geologic history of the Southern Alps is marked by the growth of extensive carbonate platforms that produced an up to 2000 m thick succession of peritidal carbonates (see Meister et al. 2013). Currently, these platforms provide the distinct character of the mountainous area from Lombardian Alps in the west to the Slovenian Julian Alps in the east (Buser 1986; Ciarapica & Passeri 1990; Borsato et al. 1994; Berra & Cirilli 1997; Ogorelec & Buser 1997; Sattler & Schlaf 1999; De Zanche et al. 2000; Bosellini et al. 2003; Gianolla et al. 2003; Galli et al. 2007; Jadoul et al. 2007; Gianolla et al. 2010; Meister et al. 2013). During the latest Triassic, the majority of these platforms belonged to the Dolomia Principale (Hauptdolomit) tidal-flat complex (e.g. Frisia 1994; Cozzi & Podda 1998; Cozzi 2002; Gianolla et al. 2003; Berra et al. 2010; Iannace et al. 2011; Meister et al. 2013). Instead, the Dachstein Limestone dominates the eastern part of the Southern Alps, now belonging to the Slovenian Julian Alps (Buser 1986; Ciarapica & Passeri 1990; Ogorelec & Buser 1997). The growth of these platform systems was strongly governed by sea-level changes. Starting with the late Carnian transgression, platform conditions became widely established during the Norian sea-level highstand (Carulli et al. 1998; Gianolla et al. 1998; Gawlick & Böhm 2000; Haas & Tardy-Filácz 2004; Pálfy et al. 2007; Krystyn et al. 2009; Berra et al. 2010; Haas et al. 2010a). The main progradation took place during the late Norian and early Rhaetian (Reijmer et al. 1991; Carulli et al. 1998; Haas & Budai 1999; Gawlick & Böhm 2000; Mandl 2000; Krystyn et al. 2009), when platform carbonates reached deeper parts of the basins (Mandl 2000).

The extent of the Dachstein Limestone has traditionally been synonymised with the extent of the Julian Platform (Buser 1989; Ogorelec & Rothe 1993; Buser 1996; Šmuc 2005; Vrabec et al. 2009), which at the time bordered the Slovenian Basin to the present south (Cousin 1981; Buser 1989, 1996; Buser et al. 2008), the Bled Basin to the present east (Cousin 1981; Goričan et

1 Geological Survey of Slovenia, Dimičeva ul. 14, SI-1000 Ljubljana, Slovenia. E-mail: luka.gale@geo-zs.si; tea.kolar-jurkovsek@geo-zs.si

2 Faculty of Natural Sciences and Engineering, Department for Geology, Privoz 11, SI-1000 Ljubljana, Slovenia. E-mail: bostjan.rozic@ntf.uni-lj.si; emencin@gmail.com

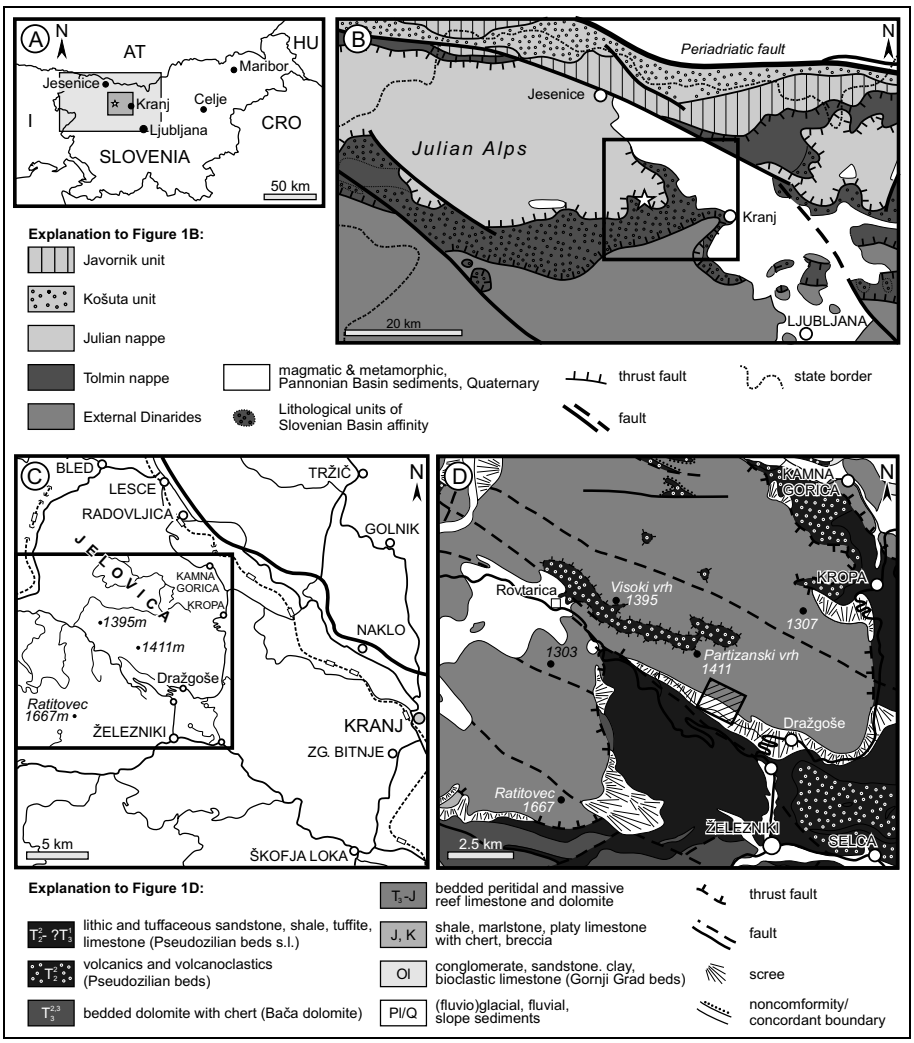

Fig. 1 - Location and geologic setting of the studied area. A) Position of figures B (light grey rectangle) and C (darker rectangle). B) Major tecto-stratigraphic units of NW Slovenia (simplified after Placer 1999). The rectangle marks the position of figure 1C. C) Location of the studied area. The area in the rectangle is enlarged in figure 1D. D) Geologic map of the Jelovica plateau (redrawn and simplified from Grad & Ferjančič 1974). The area mapped in detail in the present study (see Fig. 2) is marked by the hatched rectangle. Note that progradation near Kamna Gorica (Skaberne et al. 2003) has not been recognised by Grad & Ferjančič (1974).

al. 2012), and the Tarvisio basin to the present north (Gianolla et al. 2010; Celarc et al. 2013). The original configuration of the platform was later obscured by tectonic deformation in a collision zone between the Adriatic and European plates (Golonka 2004; Vrabec & Fodor 2006; Vrabec et al. 2006). Consequently, platform margins are rarely preserved. This is especially true at the South-Alpine thrust front, where the Julian Platform carbonates come into contact with deep-water strata of the Slovenian Basin (Placer 1999, 2008).

In this paper, we present new stratigraphic data from the southern border of the Julian Platform. The area of the Jelovica plateau (western-central Slovenia), which belongs structurally to the Krn (Julian) Nappe, is marked by transitional, basin-to-slope deposition of late Norian deeper water hemipelagics intercalated with calciturbidites. Moving upward, a thickening of the calciturbidite intercalations and a decrease in the proportion of hemipelagic limestone beds provide the first clear evidence of the late Norian progradation of the Julian Carbonate Platform towards the Slovenian Basin.

Late Triassic palaeogeography and structural subdivision of the eastern Southern Alps

The studied sections are located in the Julian Alps, which dominate the NW part of Slovenia (Fig. 1A). In the late Triassic, this area was divided into two large paleogeographic domains that originated during the Neotethys (Meliata) Ocean rifting in the middle Triassic (Vrabec et al. 2009). The deep-water Slovenian Basin was located to the present south, and most likely pinched-out to the present west (Buser 1989; Buser & Debeljak 1993; Buser et al. 2008). The northern part of the present Julian Alps belongs to the (most of the time) shallow Julian Platform (Buser 1989, 1996; Buser et al. 2008). It is connected on its western side with the larger Dinaric (Adriatic) Platform (Buser 1989; see also Cousin 1981; Rožič & Šmuc 2011) and the Dolomia Principale Platform (Gianolla et al. 2003; Meister et al. 2013).

In the eastern sector of the present Southern Alps, namely in the eastern Julian Alps, the basic NE-SW-directed late Cretaceous to Paleogene thrusting overlaps with the Neogene N-S-directed South Alpine thrusting, which provides the dominant characteristic of this area

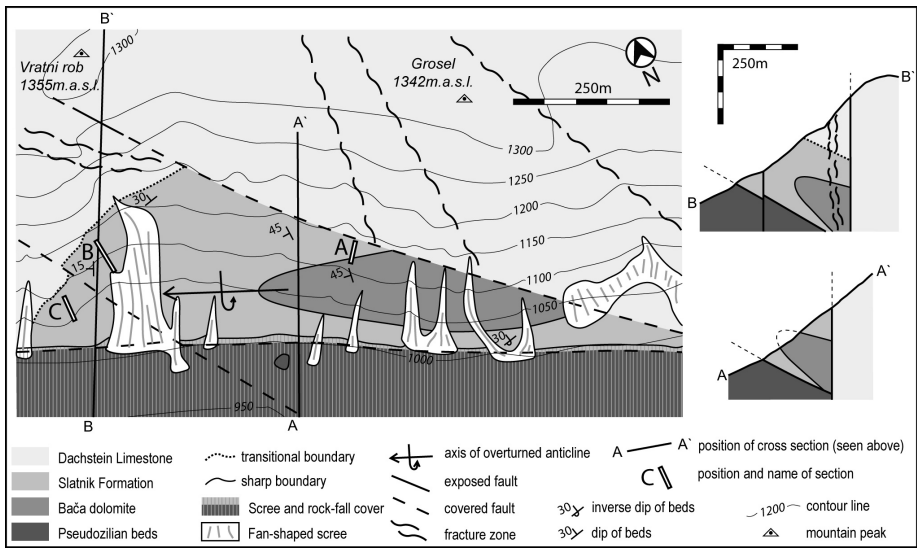

Fig. 2 - Geologic map of the studied area. White bars mark the positions of measured sections (A, B, and C).

(Doglioni & Bosellini 1987; Placer 1999; Placer & Čar 1998; Placer 2008; Kastelic et al. 2008). The Julian Alps thus comprise two large-scale thrust units, separated by a roughly west-east running Krn (Julian) thrust-fault (Buser 1986; Placer 1999, 2008). The majority of the eastern Julian Alps belongs to the upper Julian Nappe (Fig. 1B), which is composed mostly of middle to late Triassic carbonates deposited on the Julian Platform (Buser 1986, 1987; Placer 1999). The lower unit known as Tolmin Nappe is located south of the Krn thrust and composed of Slovenian Basin deposits of middle Triassic to Cretaceous age. Due to a high proportion of ductile, easily deformable clastics, the Tolmin Nappe does not form a coherent unit. Instead, it is further disintegrated into three larger subunits, the uppermost Kobla Nappe to the north, the middle Rut Nappe, and the lowermost Podmelec Nappe to the south, along with a plethora of minor internal thrusts (Buser 1987; Placer 1999). This complicated thrust-structure of the Julian Alps is further complicated by Pliocene to recent strike-slip faults (Placer 1999; Castellarin et al. 2006; Vrabec & Fodor 2006; Kastelic et al. 2008; Bavec et al. 2012; Kastelic & Carafa 2012). The transition between the Julian Platform and the Slovenian Basin is thus highly obliterated, and the proximal slope of the platform is missing.

Previous research of the studied area

The Jelovica plateau is situated at the southeastern corner of the Julian Alps and has an average altitude of approximately 1100 m above sea level (Fig. 1C). Lipold drew the first geologic map of this area around year 1859 (see Ramovš 2001). Vetters (1933) composed a geologic map based on data gathered by Teller, Kossmat, Härtel and Ampferer. A new map was later drawn by Grad & Ferjančič (1974, 1976). According to these studies, two large structural units meet in this area. The steep walls and the plateau itself belong to the Julian Nappe (Placer 1999), locally referred to as the Jelovica Nappe (e.g., Grad & Ferjančič 1976). The majority of this thrust comprises upper Triassic-Jurassic shallow water carbonates. With the exception of Lipold, who distinguished upper Triassic from lower Jurassic strata (see also Budkovič 1978), these carbonates were not further subdivided into more precisely-defined lithologic units. A minor part at the top of the Jelovica plateau is represented by volcanics, pyroclastics, marlstone and shale, which were determined as Ladinian Pseudozilian beds (cf. Pleničar et al. 2009) beds (Fig. 1D). Near Kamna Gorica (see Figs 1C, D), Carnian platform progradation over Pseudozilian beds has been recorded (Skaberne et al. 2003).

Pseudozilian beds of the second large structural unit, the Tolmin Nappe (Placer 1999), belong to a much deeper depositional milieu (Skaberne et al. 2003), i.e., a more distal part of the Slovenian Basin.

In addition, more narrowly focused research in this area was performed by Grafenauer (1980), Turnšek & Buser (1991), Turnšek (1997), Brenčič (2003), and Skaberne et al. (2003), while Zupan (1990), Zupan-Hajna (1995) and Pleničar (2000) primarily summarised data from other researchers.

Methods

The first step in this study involved the new geologic mapping of a small area 1.5 km NW of the Dražgoše village (Fig. 2). This new mapping serves to establish lateral and vertical relationships among the lithologic units ("formations") that are unknown from existing maps. Subsequently, three sedimentological sections were investigated in detail. Fifty-five thin sections were prepared from 54 samples. Thin sections are stored at the Faculty of Natural Sciences and Engineering, Department for Geology (Privoz 11, SI-1000 Ljubljana, Slovenia).

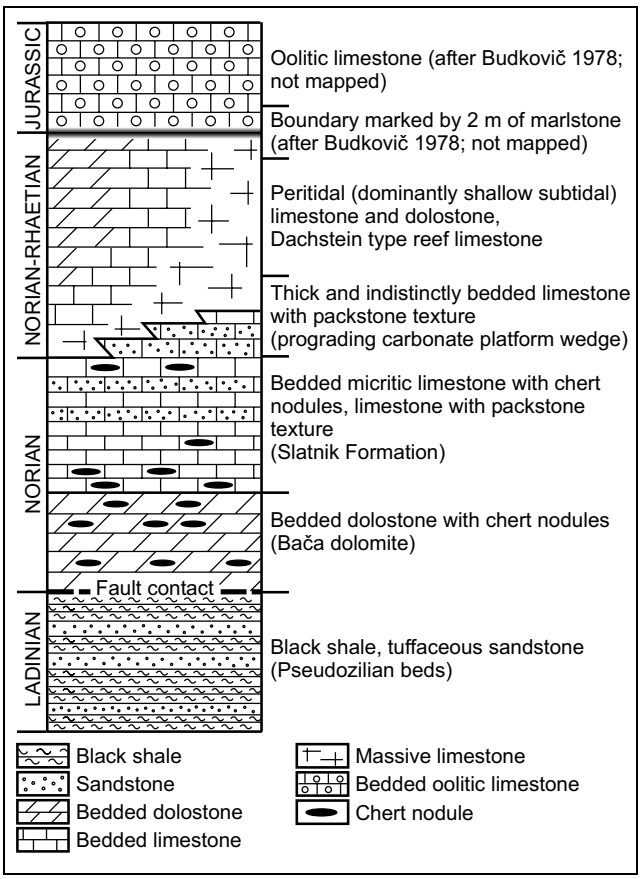

Fig. 3 - Schematic lihostratigraphic column of the southern and south-eastern Jelovica plateau.

Microfacies types are described in terms of Dunham (1962) classification. The clast proportion was determined using the charts of Baccelle & Bosellini (1965).

For very small and rounded micritic grains (peloids) in mud-dominated microfacies the term fecal pellet (Flügel 2004: 111) is used as we predict their fecal origin. In grain-dominated microfacies, peloids exhibit larger size variation. Most have clear, distinct boundaries and subangular to angular shapes. These characteristics suggest the syndepositional reworking of carbonate mud, and they are thus named mud peloids. Due to poor sorting and repeated occurrence throughout the section, the more narrow term "lithic peloids" could also be applied. Based on the arbitrarily set size limit, mud peloids larger than 200 μm are called intraclasts. Alternatively, a minor portion of the peloids in grain-dominated microfacies types possibly belongs to fecal pellets and bioerosional peloids (Flügel 2004: 113).

For the purposes of biostratigraphy, 11 samples were collected for conodont preparation, and later treated with 5% formic acid following the standard procedure. Residues are stored at the Geological Survey of Slovenia (Dimičeva ul. 14, SI-1000 Ljubljana, Slovenia) under repository numbers 5037, 5246, 5247, and 5267-5272.

Results

Geologic structure of the studied area

A small part of the southern slope of the Jelovica plateau NW of Dražgoše village was mapped anew (Fig. 2). Four lithostratigraphic units were distinguished in the field: Pseudozilian beds, Bača dolomite, the Slatnik Formation, and shallow-water (peritidal) limestone and dolostone (Fig. 3). Two major structural units have been identified. The Tolmin Nappe in the south, comprised of clastic Pseudozilian beds, forms the lower slopes of the Jelovica plateau up to an elevation of 1000 m above sea level (a.s.l.). Its northern border is indicated by a WNW-ESE verging fault (Fig. 2). The slopes above 1000 m a.s.l. and the top of the plateau belong to the Julian Nappe, which is crossed by several faults. One of these faults, which runs in a NW-SE direction, forms the northern boundary of a distinct tectonic block in which basinal carbonates (Bača dolomite and Slatnik Formation) are recumbently folded. The Julian Nappe north of this fault consists of shallow-water carbonates.

The Pseudozilian beds are characterised by black shale, lithic sandstone and tuffaceous sandstone that are mostly covered by scree and rock-fall deposits. No fossils were found in the field, and a Ladinian age is assumed on the basis of the general stratigraphy of the eastern Southern Alps (e.g. Buser 1986; Skaberne et al. 2003).

The Bača dolomite is distinguished by medium to very-thick beds of dark grey dolomicrosparite and dolosparite along with occasional nodules of black or white chert (Pl. 1, fig. 1). Parallel lamination is rarely visible. Dolomitic slump breccias with dolomitic intraclasts and brecciated chert are locally present (Pl. 1, fig. 2). This informal stratigraphic unit was described until now only for the Tolmin Nappe (Kossmat 1914; Buser 1986; Gale 2010), although Brenčič (2003) also mentioned it on the northern slopes of the Jelovica plateau.

PLATE 1

Macroscopic features of the Norian Bača dolomite and the Slatnik Formation.

Fig. 1 - Thin- to medium-thick bedded dolostone with chert nodules. Bača dolomite.

Fig. 2 - Dolostone breccia with chert clasts. Bača dolomite.

Fig. 3 - Thin- to medium-thick bedded micritic limestone with chert nodules. Arrows point in the direction of the pinching-out of two thicker beds. Slatnik Formation.

Fig. 4 - Limestone bed with two horizons and normal grading (arrowheads at the base). Packstone passing into wackestone/mudstone texture. Slatnik Formation.

Fig. 5 - A boulder of silicified coral limestone (hand) in a massive limestone bed with packstone texture. Slatnik Formation.

Fig. 6 - A meandroid colonial coral (arrowhead) and a completely silicified cockade (K) from the boulder in Fig. 5. The facing surface is directed perpendicular to bedding plane.

Fig. 7 - A silicified phaceloid colonial coral (arrowhead) and a silicified cockade (K) from the boulder in Fig. 5. The upper side of the boulder is to the left (in the direction of the point of the hammer). The facing surface is directed perpendicular to the bedding plane.

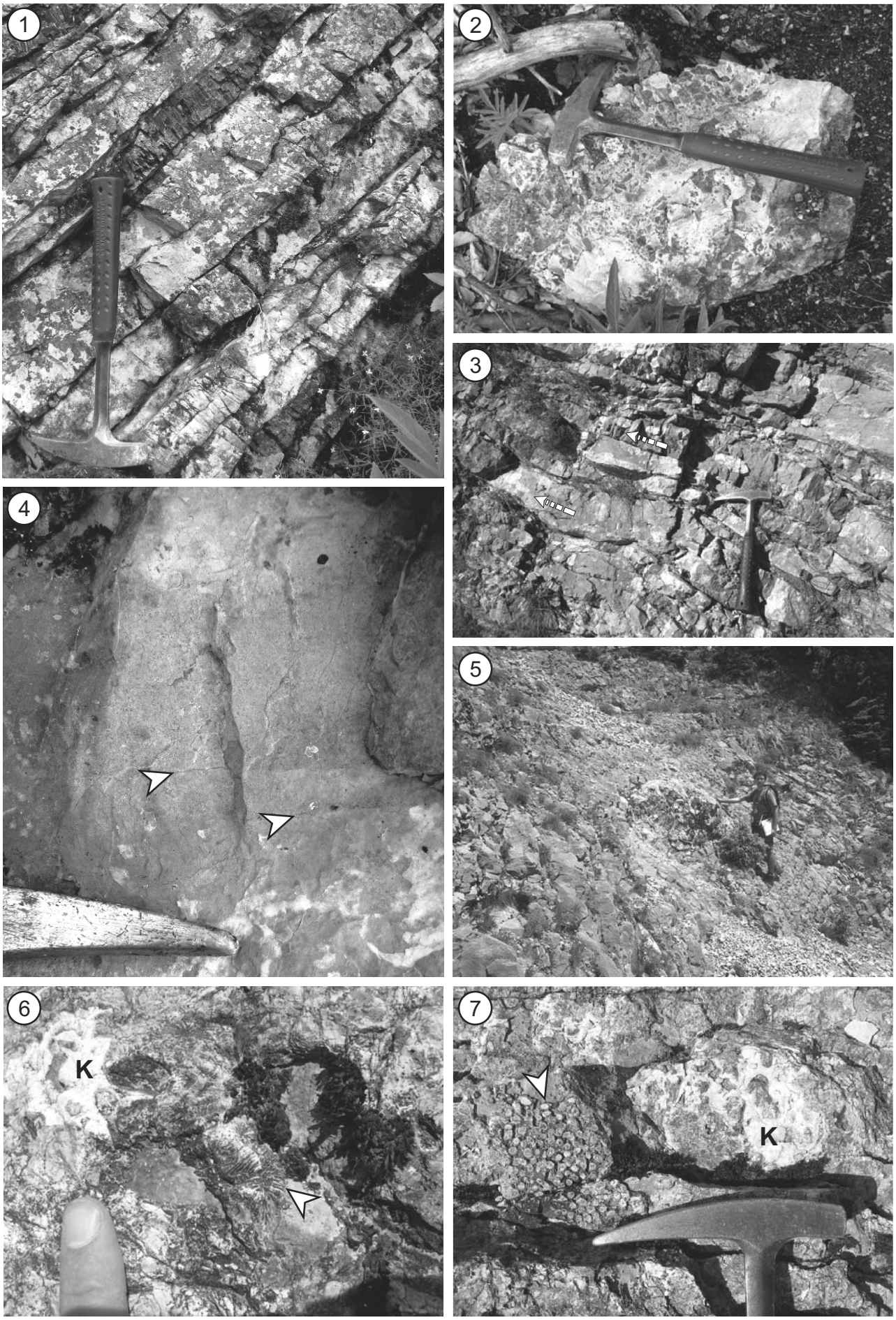
1
2
3
4
5
6
K
7
K

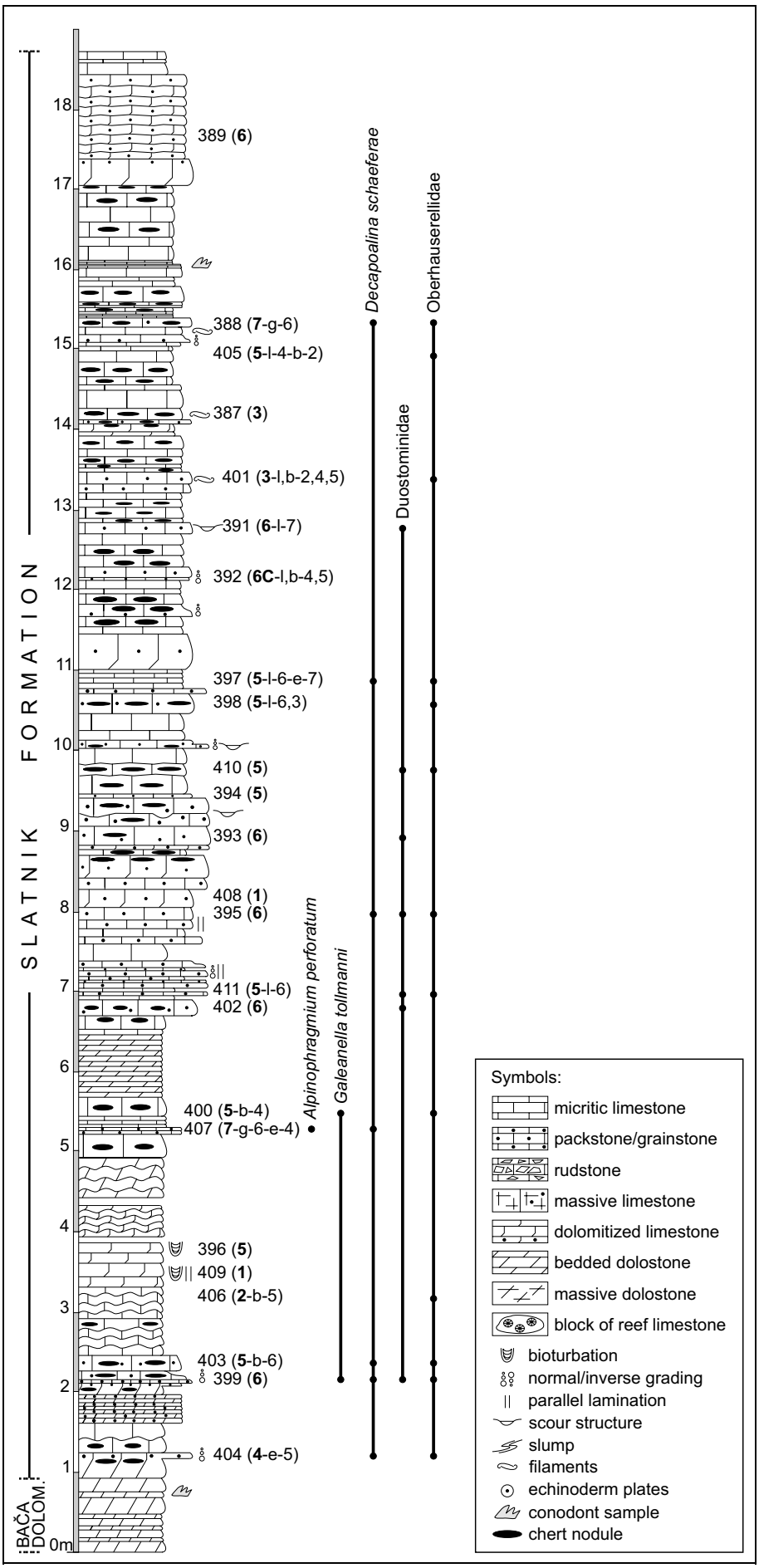

Fig. 4 - Section A. Basal part of the Slatnik Formation. Numbers at right represent the thin section numbers. Numbers in brackets indicate microfacies type (see text). Where two or more microfacies types are present within the same thin section, the dominant type is written in bold and a letter marks the contact with other types: e- erosional, b- bioturbation, g- graded, l- laminae. Important foraminiferal species are presented on the right (see Table 1 for all data).
Microfacies types: 1- mudstone, 2- radiolarian wackestone, 3- filament packstone, 4- peloidal-bioclastic wackestone, 5- very fine-grained bioclastic-peloidal packstone, 6- fine- to medium-grained bioclastic-peloidal grainstone (subtype 6C- with abundant micritic envelopes), 7- lithoclastic-bioclastic-intraclastic grainstone/rudstone.

The Bača dolomite is succeeded by the Slatnik Formation, i.e., bedded limestone with or without chert nodules (Pl. 1, fig. 3). Thin to medium-thick bedded mudstone, wackestone and packstone/grainstone predominate in the lower part of the unit. Thick and very-thick bedded packstone/grainstone (Pl. 1, fig. 4) are more common higher up in the succession, where it is interchanged with 30-40 cm thick packages of thinner beds; slumps are also present. The Slatnik Formation has been known until present only from the Tolmin Nappe, where it was dated as late Norian to end-Rhaetian in age (Rožič 2008; Rožič et al. 2009; Gale et al. 2012; Rožič et al. 2013). Upper Triassic limestone with chert NE of the Ratitovec summit was mentioned by Pleničar (2000). However, a detailed description was not provided.

Peritidal carbonates, which form the major part of the Julian Nappe north of the studied area, are represented by massive reef limestone, thick and very-thick bedded limestone with mudstone, wackestone, packstone/grainstone and (rarely) bindstone (i.e., stromatolitic texture), as well as thick to very-thick bedded dolostone. According to corals identified at other localities (Turnšek & Buser 1991; Turnšek 1997), this unit is Norian and Rhaetian in age. However, a Carnian or even late Ladinian age was determined further to the east (Grad & Ferjančič 1976; Skaberne et al. 2003).

Description of the Slatnik Formation

The Slatnik Formation was investigated in detail in three sections (Fig. 2):

• *Section A* (N 46°15'48", E 14°09'07"; Fig. 4) encompasses the basal part of the Slatnik Formation. This section starts with thin to medium-thick bedded Bača dolomite followed by partly-dolomitised limestone bed with packstone/grainstone texture and normal grading. Thin-bedded fine grained packstone/grainstone and mudstone then interchange through the section. Limestone is occasionally dolomitised and exhibits planar or nodular bedding. Parallel lamination, bioturbation, and normal grading are rarely visible. Scour structures are evident as laterally restricted packstone/grainstone beds (Pl. 1, fig. 3). In addition to the already-mentioned textures, the upper third of the section also contains packstone with filaments. Chert nodules are present throughout the section; their distribution does not seem to be selective to bed thickness or texture.

• *Section B* (N 46°15'51", E 14°08'45"; Fig. 5) was measured along the dry channel ending on top of the scree. This section represents the upper part of the Slatnik Formation. Black thin- and medium-thick bedded, normally graded coarse grainstone predominates in the lower 15 m. Chert nodules are rarely present and amalgamation is common. Two very-thick beds have scoured bases. Up to 1.5 m large boulders of strongly silicified reef limestone were found in the upper one (Pl. 1, fig. 5). Corals are of the meandroid and faceloid types and are randomly oriented (Pl. 1, figs 6-7). Cockades are completely replaced by silica. Grainstone surrounding the boulders contains small and dispersed silicified bivalve shells with no preferable orientation with respect to the bedding. Over the next 6 m (metres 15 to 20 in Fig. 5), medium-thick beds of black mudstone and wackestone are prevalent while fine-grained packstone/grainstone is subordinate. From the 20th metre up, thin- and medium-thick packstone/grainstone again predominates and normal or inverse grading is locally visible. Some beds have scoured bases, or show synsedimentary deformation (slumping). Another very-thick grainstone bed between metres 26 and 27 contains isolated limestone boulders. Lateral thinning is evident, and the base is most likely scoured. From 27th to 34th metres, thin- to medium-thick limestone with mudstone and wackestone textures are again predominant, and chert nodules are a bit more abundant. Thinner, laterally pinching-out layers of normally graded packstone/grainstone occasionally interrupt the interval. The lithology abruptly changes at the 34th metre of the section; very-thick beds of light gray limestone and dolostone with packstone/grainstone texture start to prevail. Although the transition itself is poorly exposed due to dolomitisation, it appears structurally undisturbed. Bedding is hardly discernible. Mudstone and wackestone are rarely present, occurring mostly in horizons with no distinct bedding. The texture is generally massive, with only one case of normal grading.

• *Section C* (N 46°15'51", E 14°08'45"; Fig. 6) is positioned approximately lateral to Section B. Thin to middle-thick beds with mudstone and wackestone textures interchange with packstone/grainstone in the lower part of the section. Beds are internally amalgamated, and the bedding is somewhat nodular. Nodules of black chert are common. Normal grading is rarely present in the packstone/grainstone (Pl. 1, fig. 4), and one bed with a scoured bottom was recognised around the 11th metre. After the 17th metre, medium- to very-thick bedded packstone/grainstone that is often normally graded begins to predominate. Chert nodules are completely absent, even in the rare wackestone beds. Bedding planes become indistinct, and internal amalgamation further renders determination of bed boundaries difficult.

Microfacies analysis

From the 54 samples collected along the measured sections of the Slatnik Formation, seven microfacies (MF) types are described. Their distribution along the sections is presented in Figures 4-6.

The first four MF have mud-supported textures, while the last three have grain-supported textures. The

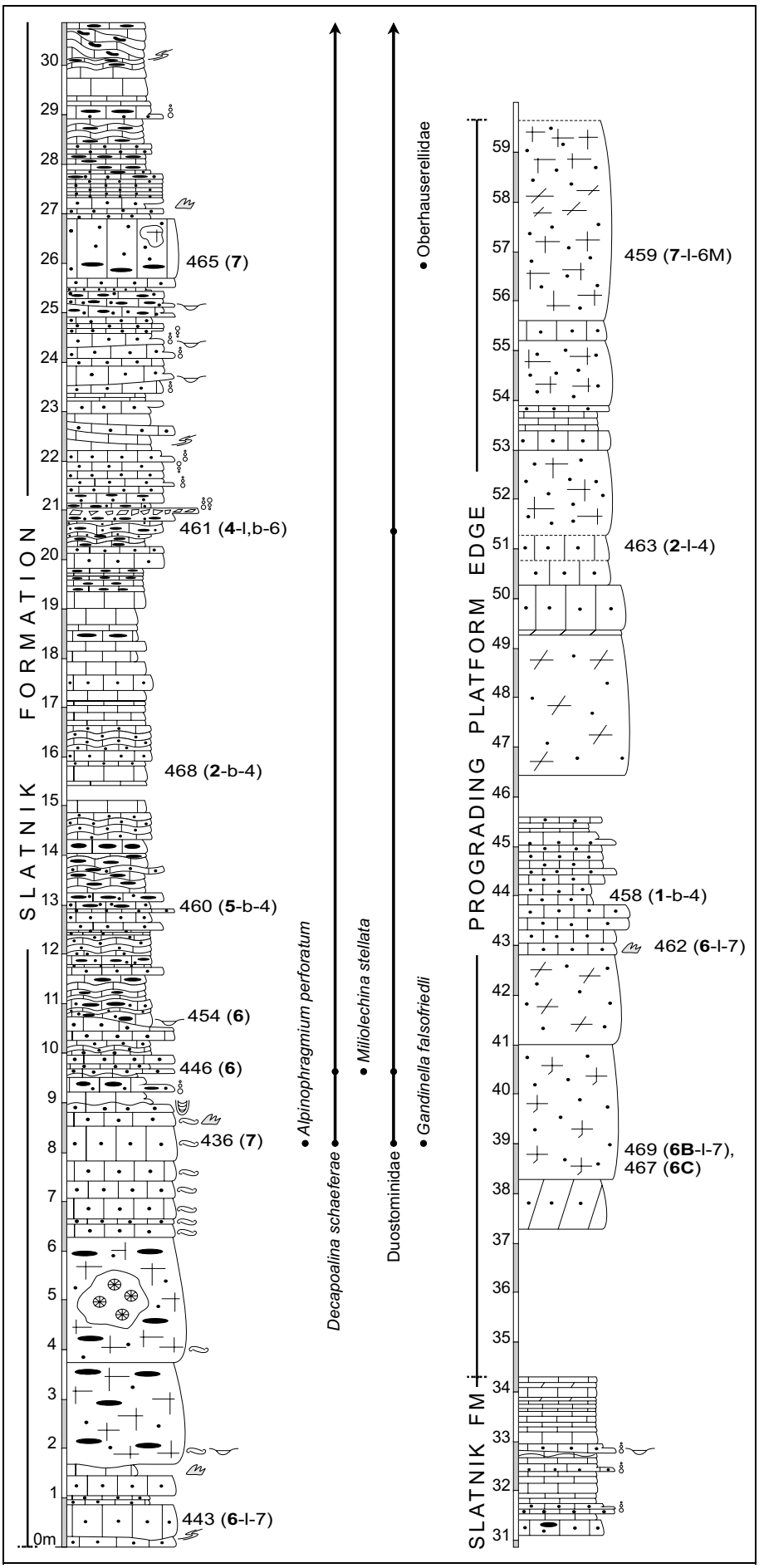

Fig. 5 - Section B. Upper part of the Slatnik Formation. Numbers to the right represent thin section numbers. Numbers in brackets indicate microfacies type (see text). Where two or more microfacies types are present within the same thin section, the dominant type is written in bold and a letter marks the contact with other types: b- bioturbation, l- laminae. Important foraminiferal species are presented on the right (see Table 2 for all data). For legend see Figure 4 or 6.
Microfacies types: 1- mudstone, 2- radiolarian wackestone, 4- peloidal-bioclastic wackestone, 5- very fine-grained bioclastic-peloidal packstone, 6- fine- to medium-grained bioclastic-peloidal grainstone (subtype 6B- with high abundance of bivalve shell fragments; subtype 6C- with abundant micritic envelopes; subtype 6M- with abundant micritic envelopes and calcimicrobes), 7- lithoclastic-bioclastic-intraclastic grainstone/rudstone.

transition from one MF type to a similar one can take place over a distance smaller than the thin-section size. This change is usually related to grading, alternating lamina, bioturbation or erosion. Dolomitisation and silicification are locally present irrespective of MF type, and are thus described after the description of each MF type.

• *MF 1: Mudstone* - This MF type (Pl. 2, fig. 1) is homogenous in structure and composition. Fine grained micritic matrix predominates. Fecal pellets and fine bioclasts are very rare (2.5%), and echinoderms and filaments are present.

• *MF 2: Radiolarian wackestone* - The texture is homogenous or even-laminated with laminae up to 8 mm thick. Laminae are defined by varying grain-contents which typically do not exceed 30%. Lower boundaries of the laminae are sharp, while upper boundaries are gradual. Grains mostly comprise small bioclasts (90% of grains) and fecal pellets (10%), and grain size is usually less than 200 μm. Radiolaria are the most common among bioclasts (Pl. 2, fig. 2). Small echinoderm plates, filaments (thin-shelled bivalves), small foraminifera (mostly Oberhauserellidae), ostracods, sponge spicules, and unrecognisable debris are subordinate. One sample from the upper part of Section B contained more abundant sponge spicules. Bioturbation was detected in all thin sections. The texture in large burrows is typically homogenised and clearly distinct from the surrounding sediment. In some thin sections bioturbation completely obliterates primary lamination. Rare laminae have a very fine-grained packstone texture and contain more abundant fecal pellets.

• *MF 3: Filament packstone* - This MF exhibits a bimodal grain-size distribution: larger grains (up to 2 mm long) belong to filaments (Pl. 2, fig. 3), whereas other grains are typically smaller than 200 μm. This MF type commonly alternates in laminae with MF 2 and MF 4. The ratio between grains varies, but filaments usually compose at least 50% of the total grain surface. Filaments are often oriented parallel to bedding to form shelter textures, which are particularly expressed when they are orientated convex-upwards. The sheltered parts are partly filled with spar. Where filaments are prevalent, a prominent recrystallisation is observed in which subhedral large crystals (up to 30 μm large) of spar are concentrated in vertical columns. Because the filaments

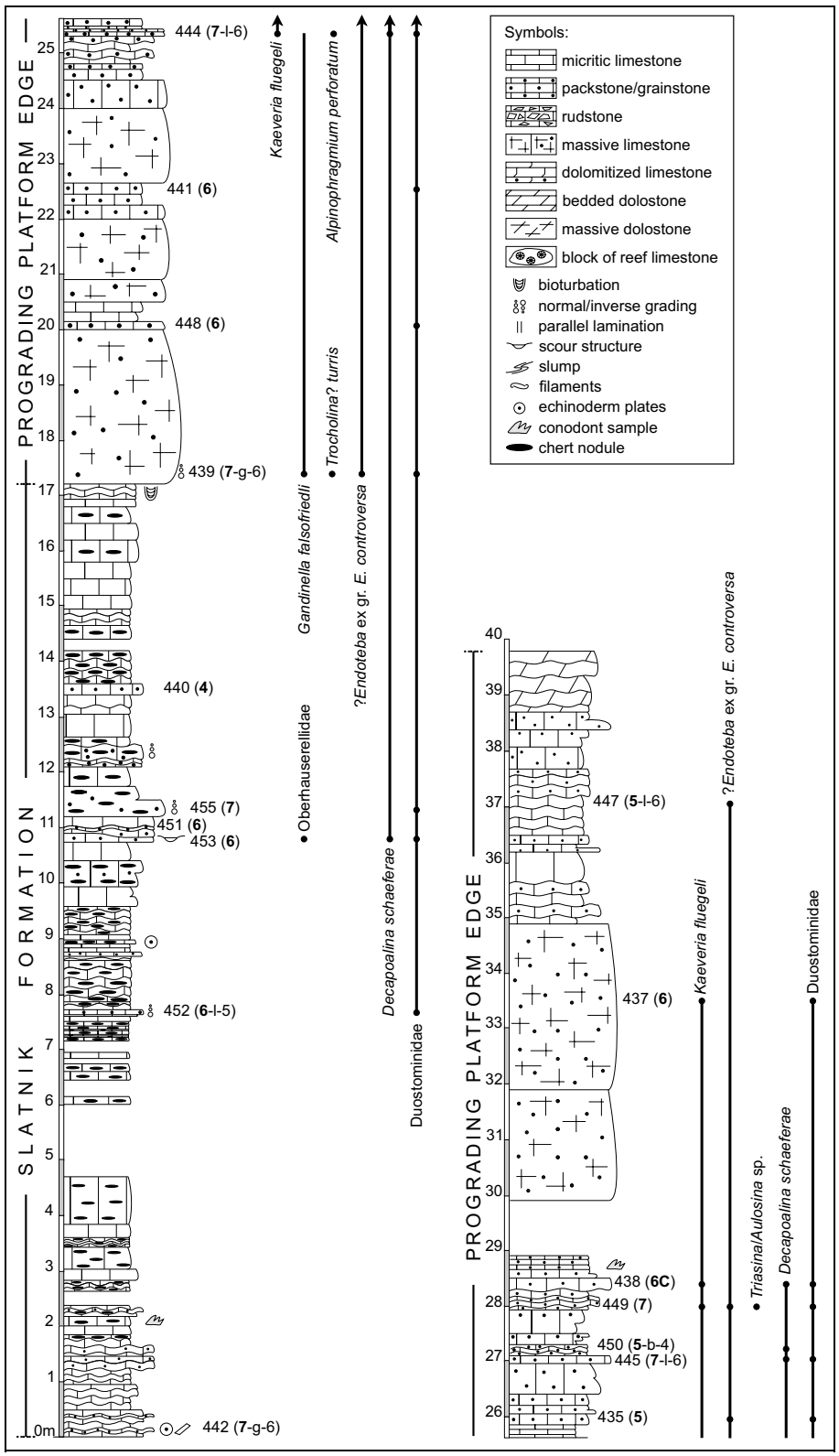

Fig. 6 - Section C. Upper part of the Slatnik Formation. Numbers to the right represent thin section numbers. Numbers in brackets indicate microfacies type (see text). Where two or more microfacies types are present within the same thin section, the dominant type is written in bold, and the contact with other types marked by a letter: b- bioturbation, g- graded, l- laminae. Important foraminiferal species are presented to the right (see Table 2 for all data).
Microfacies types: 4- peloidal-bioclastic wackestone, 5- very fine-grained bioclastic-peloidal packstone, 6- fine- to medium-grained bioclastic-peloidal grainstone (subtype 6C- with abundant micritic envelopes), 7- lithoclastic-bioclastic-intraclastic grainstone/rudstone.

are often bent upward along these features, we relate these textures to the water-escaping tubes; alternatively, they could represent burrowing. Intergranular spaces among filaments are filled with very-fine-grained packstone in which fecal pellets and small intraclasts prevail (over 90% of small clasts). Other grains are echinoderm plates (approximately 5% of the fine-grained component), neomorphically-altered fragments of mollusc shells (2.5%), rarely with micritic envelopes, and rare foraminifera (mostly Lagenina and Miliolina).

• *MF 4: Peloidal-bioclastic wackestone* - Peloidal-bioclastic wackestone shows homogenous and in-part bioturbated texture. Grains represent up to 40% of area (Pl. 2, fig. 4). They have the same composition as MF 2 but are generally larger in size (up to 0.5 mm). Echinoderm plates, calcified radiolaria and sponge spicules prevail among bioclasts, which typically represent 90% or more of the total grain number, but whose proportion can decrease also below 10% of the total grain number. Ostracods, foraminifera and fragmented filaments can also be locally common, while gastropods and mollusc fragments with lamellar or columnar crystal-arrangements are always subordinate in number. Peloids (likely fecal pellets) are mostly rare, but can amount up to 90% of grain count at the expense of bioclasts. Some thin sections contain large (up to 3 mm) ovular and slightly elongated fields filled with spar and sometimes containing microquartz in the centre. These fields are presumably recrystallised, and occasionally contain silicified bioclasts.

• *MF 5: Very-fine-grained bioclastic-peloidal packstone* - This MF type is homogenous with well-sorted grains or evenly laminated texture. Grains represent 50% of the thin section area (Pl. 2, fig. 5, 6). Intergranular space is filled with micritic matrix, which may have been partly winnowed away. These interstices were later filled with blocky spar. Grain size is mostly 100-180 μm, with exceptions reaching 300 μm; some filaments or echinoderm plates, however, can be up to 1.8 mm in size. Mud peloids are prevalent (90% of total grain number) followed by echinoderm plates (5%), and cortoids (i.e., neomorphically-altered mollusc shells with micritic outline (3.5%). Foraminifera, brachiopod fragments, ostracods and other bioclasts as well as small, mostly micritised ooids are less abundant. Filaments are locally more abundant in some laminae.

• *MF 6: Fine- to medium-grained bioclastic-peloidal grainstone* - The grainstone is texturally homogenous, although partly-washed-out packstone (MF 5) can also be encountered in the same thin section. Gradation (average grain size ranging from 150-200 μm to 250-350 μm) and parallel lamination are sometimes visible. Fine-grained variety exhibits good sorting, whereas sorting turns poor in the medium-grained subtype. Grain proportion is approximately 50%, and elongated grains are oriented parallel to bedding. Shells can form shelter and geopetal textures (Pl. 2, fig. 7). Intraclasts predominate in this MF type (74% of total grain number). A few exhibit wackestone, fine-grained peloidal or bioclastic-peloidal packstone textures; however, the majority is completely micritised. Micritic intraclasts smaller than 200 μm are termed mud peloids. Micritic grains are usually sub-rounded and isometric to elongate.

Bioclasts are subordinate in number (up to 25% of grains), as are small, radial ooids (0.5%). Among bioclasts, echinoderms are prevalent (9% of grains). Foraminifera are also common (1% of grains), whereas ostracods, fragments of mollusc and brachiopod shells, small gastropods, calcimicrobes, calcisponges, microproblematica (*Baccanella* sp. and *Bacinella* sp.) and neomorphically-altered dasycladacean geniculi occur only sporadically. In some thin-sections, some grains are encrusted by microbialites and foraminifera. The micritic envelopes of bioclasts (i.e., cortoids) are quite common in some samples; this variety is marked as number 6C in Figures 4-6. In the uppermost part of the Slatnik Formation (Section B), cortoids co-occur with the more abundant calcimicrobial grains that also show micritic edges; this variety of MF 6 is marked as 6M in Figure 5. The third variety, also encountered in the upper part of the Slatnik Formation and marked as 6B (Fig. 5), has a distinct high abundance of bivalve shell fragments.

• *MF 7: Lithoclastic-bioclastic-intraclastic grainstone/rudstone* - This MF is characterised by a bimodal grain size distribution where pebble-sized (up to 10 mm) grains are supported by grainstone (Pl. 2, fig. 8), which is the same as in MF 6.

Pebble-sized grains are sorted in three major clast-groups. The first comprises large echinoderm plates, bivalve shells, rarer calcisponges, and calcimicrobes. Two shell types were recognized; in the first type, the thinner outer layer is foliated, whereas the thicker inner layer is prismatic. These layers may successively alternate in a few multilayered fragments. The second type of shells is characterised by a thicker, inner foliated layer followed by a thin, prismatic outer layer. In one of the samples, elongated, isolated patches of spar up to 4 mm in size occur within the grainstone. These patches have indistinct boundaries, and spar infilling displays a general increase in crystal-size moving towards the centre. These features indicate the cement infill of a void. We interpret these patches as either completely dissolved and neomorphically-replaced shells or bioturbation fillings.

The second clast-group includes well-rounded clasts with textures and compositions corresponding to the previously described MF types; these clasts are thus interpreted as intraclasts. Microfacies types 2 and 4 predominate, although clasts of MF 5 are also observed. A 1 cm large, spherical clast was observed in a sample from the upper part of Section C with a composition and texture corresponding to MF 4; however, it also exhibits a concentric inner structure. Alternating laminae differ in the amount of bioclasts, which become more abundant in outer laminae. Edges of this clast show plastic deformation, thus, it could also be interpreted as a poorly lithified oncoid.

The third clast-group comprises lithoclasts of the following types: (a) boundstone with alternating crusts of microbialites and microproblematica *Bacinella*; (b) wackestone (rarely passing to packstone) similar to MF 4, but with rare, large (up to a few millimeters) echinoderm plates, bivalve fragments and foraminifera; (c) intraclastic-bioclastic wackestone with framboidal pyrite, bioclasts (echinoderms and fragments of molluscs), and intraclasts (recrystallised peloidal-bioclastic wackestone); (d) coarse-grained peloidal-bioclastic grainstone with neomorphically-altered bivalve shell fragments with micritic outlines, echinoderms, foraminifera, gastropods, calcimicrobes, and rare juvenile ammonite as bioclasts; (e) partly washed-out packstone with a large two-layered shell, encrusted by foraminifera, intraclasts and foraminifera; (f) bioclastic-peloidal grainstone with common foraminifera; and (g) peloidal wackestone/packstone with a pseudospar matrix.

Common diagenetic features. Some diagenetic features appear independent of MF type. The most

PLATE 2

Microfacies types of the Slatnik Formation.

Fig. 1 - Mudstone with rare bioclasts (MF 1). Thin section 408.

Fig. 2 - Radiolarian wackestone-packstone (MF 2). Thin section 439.

Fig. 3 - Filament packstone (MF 3). Thin section 457.

Fig. 4 - Peloidal-bioclastic wackestone (MF 4). Thin section 460.

Fig. 5-6 - Very fine-grained bioclastic-peloidal packstone (MF 5). Thin sections 435 and 394, respectively.

Fig. 7 - Fine- to medium-grained bioclastic-peloidal grainstone (MF 6). Note the geopetal texture in the bivalve shell. Thin section 391.

Fig. 8 - Lithoclastic-bioclastic-intraclastic grainstone/rudstone (MF 7). Thin section 469.

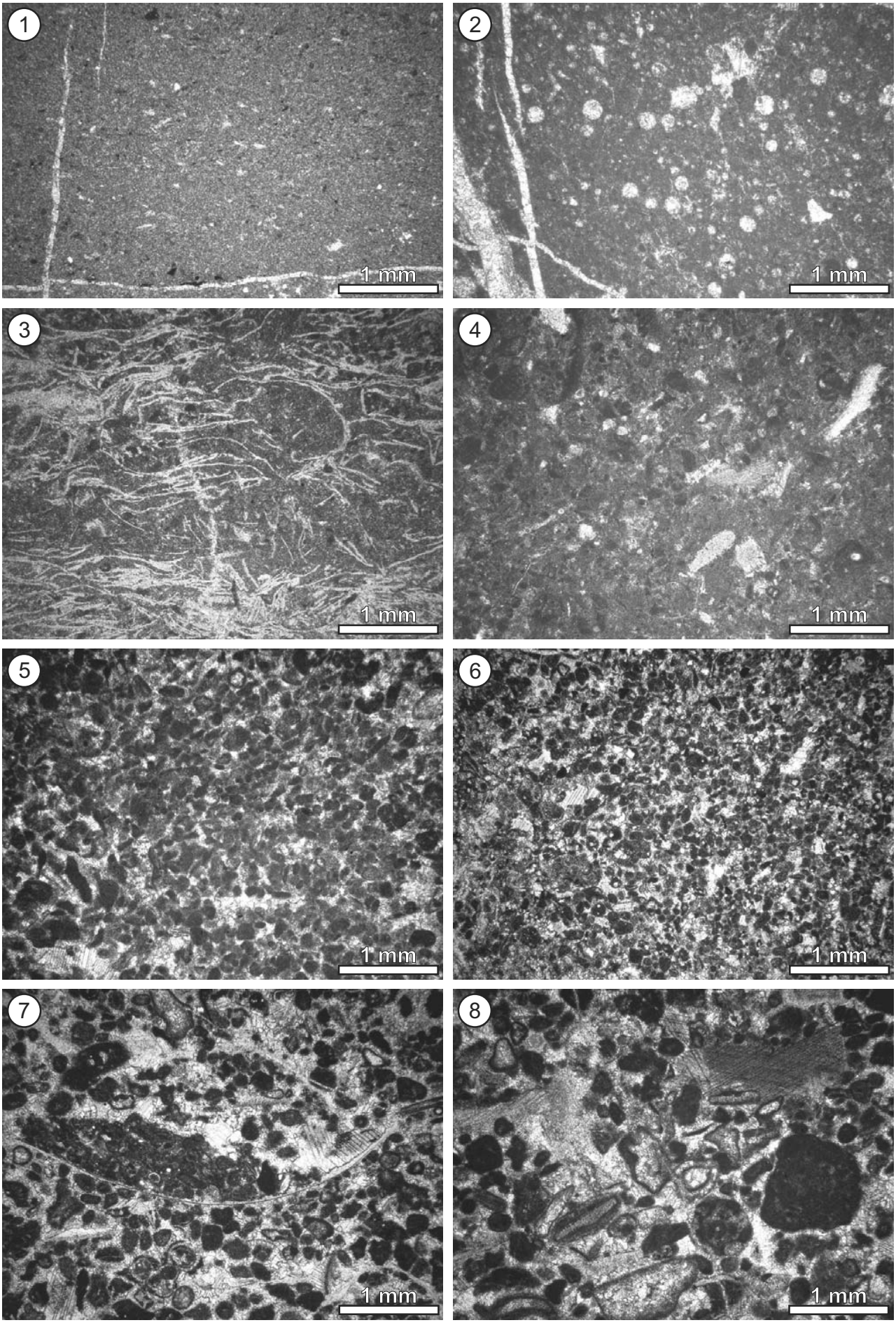
1
1 mm
2
1 mm
3
1 mm
4
1 mm
5
1 mm
6
1 mm
7
1 mm
8
1 mm

	404	399	403	406	409	396	407	400	402	411	395	408	393	394	410	398	397	392	391	401	387	405	388	389
Alpinophragmium perforatum							+																	
?*Duotaxis birmanica*		+																						
Verneuilininae																	+							
Reophax rudis																			+					
Ammobaculites in *Reophax*		+					+		+	+	+		+				+						+	+
»*Trochammina*« *almtalensis*		+						+							+		+							
»*Trochammina*« *jaunensis*								+									+							
Earlandia tintinniformis																							+	
Endotriada tyrrhenica											+													
Endothyroidea		+							+															
Planiinvoluta carinata											+													
Ophthalmidium sp.		+						+		+	+					+	+							
Galeanella tollmanni		+						+																
Miliolipora tamarae																		+	+					
?*Cucurbita infundibuliformis*								+																
Agathammina austroalpina		+	+	+			+	+		+	+									+			+	
Decapoalina schaeferae	+	+	+				+				+						+						+	
Duostominidae		+							+	+	+		+		+				+					
Variostoma coniforme											+													
Oberhauserellidae	+	+	+	+				+		+	+				+	+	+			+		+	+	
Lagenina	+	+	+			+		+	+	+	+				+		+	+		+		+	+	

Tab. 1 - Distribution of foraminifera (vertical axis) in thin sections (horizontal axis) from Section A.

	443	436	446	454	460	468	461	464	465	469	462	458	463	459	442	452	453	451	455	440	439	448	441	444	435	445	450	449	438	437	447
Tolypammina sp.		+						+	+	+																					
Gandinella falsofriedli		+																			+			+							
Kaeveria fluegeli																								+				+	+	+	
Alpinophragmium perforatum		+																						+							
?*Duotaxis birmanica*															+						+										
Duotaxis metula			+																												
Verneuilininae																								+							
Reophax rudis	+	+	+					+						+					+									+			
Ammobaculites ali *Reophax*			+	+					+	+	+				+			+			+	+		+		+		+	+		
»*Trochammina*« *almtalensis*														+				+													
»*Trochammina*« *jaunensis*																															+
Endotriada tyrrhenica					+													+							+						
?*Endoteba controversa*																					+				+			+			+
Endothyroidea			+	+														+				+		+				+			
Trocholina? *turris*																					+										
Aulotortus sinuosus										+														+							
Aulotortus friedli																								+							+
?*Aulosina oberhauseri*																												+			
Ophthalmidium sp.	+		+	+						+				+										+							
?*Miliolipora cuvillieri*									+																						
Miliolipora tamarae	+		+																												
Agathammina austroalpina			+														+		+					+							
Decapoalina schaeferae		+	+								+			+			+							+		+	+		+		
Miliolechina stellata			+																												
Duostominidae		+	+				+	+		+	+					+	+		+		+	+	+		+	+		+	+	+	
?*Variostoma cochlea*														+																	
Variostoma coniforme		+															+					+	+	+	+					+	
Oberhauserellidae									+								+														
Lagenina		+		+				+		+	+				+	+	+		+	+	+	+	+				+	+	+		

Tab. 2 - Distribution of foraminifera (vertical axis) in thin sections (horizontal axis) from Section B (left of the double vertical line) and Section C (right from the double vertical line).

common of these are dolomitisation and silicification. Dolomitisation occurs in form of dispersed sub- to euhedral crystals (usually up to 200 μm large), which tend to replace micrite in either matrix or in grains. The process seems more intense in the lower part of the Slatnik Formation, where the dolostone completely replaces individual laminae or is concentrated in ovular fields up to a few millimeters in size. The transition from this intensely dolomitised rock into unaltered rock is gradual. Some of the dolostone patches were interpreted as selectively-replaced mudstone/wackestone intraclasts. Silicification occurs in the form of chert nodules. In thin-section, selective replacement of bioclasts by fibrous or microgranular quartz was rarely observed.

Other diagenetic features include recrystallisation to microsparite in matrix-containing MF types 1 to 5, and crystallisation of framboidal pyrite.

Biostratigraphy

The age of the Slatnik Formation is determined on the basis of benthic foraminifera (more abundant in packstone), and conodont elements. While Triassic foraminifera generally have rather broad stratigraphic ranges, dating with conodonts provides much better resolution.

Foraminifera are relatively few in number; altogether, 23 species were determined (Pls 3-5). Their distribution in thin sections is reported in Tables 1 and 2. The species of stratigraphic importance are *Decapoalina schaeferae* (Zaninetti et al.), *Galeanella tollmanni* (Kristan) and *Alpinophragmium perforatum* Flügel. Their stratigraphic range is restricted to the Norian and Rhaetian (see Gale 2012a, with references). The specimen figured on Plate 4, figure 14 and determined as *Triasina/Aulosina* sp. matches specimens determined by Gale (2012b) and Gale et al. (2012) as *Triasina oberhauseri* Koehn-Zaninetti (in Koehn-Zaninetti & Brönnimann). *Triasina oberhauseri* (*Aulosina oberhauseri* according to Rigaud et al. 2013) differs from *Triasina hantkeni* Majzon because of its smaller test, fewer coilings, and higher chamber lumen. The upper stratigraphic range of *Aulosina oberhauseri* is late Norian (Gale 2012b; Rigaud et al. 2013), while *Triasina hantkeni* corresponds only to the Rhaetian (Grgasović 2003; Velić 2007; Gale et al. 2012; Rigaud et al. 2013), although some researchers also consider it late Norian in age (Oravecz-Scheffer, 1987; Martini et al. 2004; Mancinelli et al. 2005; Krystyn et al. 2007).

Conodont elements were recovered from all three sections. The distribution of samples is shown in Figures 4-6. The Conodont Alteration Index is 6-7, pointing to a rather high thermal degradation of elements. *Epigondolella bidentata* Mosher is the most common element in the assemblage. It was recovered from the lower and upper parts of all measured sections. This element narrows the depositional time span of the Slatnik Formation to late Norian, i.e., Sevatian (Kolar-Jurkovšek 1991; Buser et al. 2008; Krystyn et al. 2009; Mazza et al. 2012). *Norigondolella steinbergensis* (Mosher) is present as a single specimen in the basal part of Section A, i.e., at the base of the Slatnik Formation. According to Buser et al. (2008), this species ranges throughout the Norian, while Krystyn et al. (2009) consider it middle Norian to Rhaetian in age. The first occurrence in middle Norian is also advocated by Mazza et al. (2012). The second most common element, present from the base of the Slatnik Formation and from the topmost measured part (the upper part of Section B), is *Epigondolella postera* (Kozur & Mostler). Buser et al. (2008) suggest that it ranges throughout the Norian, while Krystyn et al. (2009) restrict it to the middle Norian. The possibility of reworking seems unlikely, because the majority of samples were collected from limestone with mudstone or wackestone textures; thus, we adopt the entire Norian age after Buser et al. (2008). *Epigondolella abneptis* (Huckriede) is present only in the upper part of Section A. As for *Epigondollela postera*, its range is either late Carnian to late Norian (Buser et al. 2008) or middle Norian (Krystyn et al. 2009).

Discussion

Facies interpretation

The microfacies types encountered in the measured sections of the Slatnik Formation are comparable to those already known from sections of the Tolmin Nappe west of the studied area (Rožič 2006; Rožič et al. 2009; Gale 2012b).

Mudstone (MF 1) with rare pelagic elements corresponds to Standard Microfacies Type (SMF) 1, deposited in a basinal deep-water environment (Flügel 2004). This interpretation is further supported by radiolarian wackestone (MF 2) and filament packstone (MF 3), both belonging to the SMF 3 of Flügel (2004). Radiolaria and filaments (i.e., thin-shelled bivalves) represent open-marine biota, indicating deposition in a basinal setting (Watts 1987; Reijmer et al. 1991; Maurer et al. 2003). Concordant orientation of shells suggests either resedimentation via bottom currents or compaction (Kidwell & Bosence 1991: 154; Tucker 2003: 167). The close association of thin-shelled bivalves and peloids in MF 3 can be explained by their similar settling rates (Maurer et al. 2003) and suggests agitated bottom water rather than compaction for the cause of concordant shell orientation. The deep-water character of peloidal-bioclastic wackestone (MF 4) is likewise expressed via large contents of radiolaria, spicules and fecal pellets; mollusc fragments, however, are an allochthonous plat-

form-derived component, presumably transported into the basin by turbidity currents (see Reijmer et al. 1991; Flügel 2004: 483). Analogies to SMF 2 can be drawn (see Flügel 2004). Intense bioturbation indicates oxygenated sediments (Brenchley & Harper 1998), and stronger current activity is evident in the very-fine-grained bioclastic-peloidal packstone through partial winnowing of the mud matrix. Mud peloids, cortoids, benthic foraminifera, brachiopod fragments, and ooids were derived from the platform rim and top (see Reijmer et al. 1991) via turbidity currents. The same interpretation is suggested for fine- to medium-grained bioclastic-peloidal grainstone (MF 6) and lithoclastic-bioclastic-intraclastic grainstone/rudstone (MF 7). All three varieties (MF 5-7) can be regarded as distal turbidity deposits corresponding to SMF 4 or 5 (Flügel 2004). This interpretation is supported by the depositional textures, namely normal grading and parallel lamination (Watts 1987; Reijmer et al. 1991; Iannace et al. 1994; Tucker 2001). An increase in the proportion of lithoclasts and spar cement in calciturbidites has been explained by more proximal position (Maurer et al. 2003). Inverse-graded packstone/grainstone could represent modified grain-flow deposits (Watts 1987). According to Schlager et al. (1994) and Reijmer et al. (2012), hardened peloids form the bulk of grains during times of flooded platform top, which is in agreement with a the high sea-level during the Norian (Reijmer et al. 1991; Gianolla et

PLATE 3

Foraminifera from the Slatnik Formation

Fig. 1 - *Gandinella falsofriedli* (Salaj, Borza & Samuel). Thin section 444.

Figs 2-3 - *Kaeveria fluegeli* (Zaninetti, Altiner, Dager & Ducret). 2) Longitudinal section. Thin section 449. 3) Transverse section. Thin section 444.

Fig. 4 - *Alpinophragmium perforatum* Flügel. Thin section 407.

Figs 5-7 - ? *Duotaxis birmanica* Zaninetti & Brönnimann, in Brönnimann, Whittaker & Zaninetti; axial section. 5) Thin section 439. 6) Thin section 467. 7) Thin section 399.

Fig. 8 - ? *Duotaxis metula* Kristan; axial section. Arrowhead points at a short keel on the outer surface of the test. Thin section 446.

Fig. 9 - Verneuilininae. Thin section 444.

Figs 10-11, 13 - ? *Reophax rudis* Kristan-Tollmann. 10) Thin section 449. 11) Thin section 446. 13) Thin section 464.

Fig. 12 - *Reophax rudis* Kristan-Tollmann. Mark the offset of the initial chamber from the direction of later growth (see Kristan-Tollmann 1964). Coarsely agglutinated wall is clearly visible. Thin section 43.

Figs 14-17 - *Ammobaculites*. 14) Thin section 388. 15) Thin section 444. 16-17) Thin section 451.

Fig. 18 - "*Trochammina*" *jaunensis* Brönnimann & Page. Thin section 397.

PLATE 4

Foraminifera from the Slatnik Formation

Fig. 1, 4 - *Endotriada tyrrhenica* Vachard, Martini, Rettori & Zaninetti. Equatorial section. 1) Thin section 451. 4) Thin section 460.

Fig. 2 - Endothyracea. Thin section 447.

Figs 3, 5-9 - ? *Endoteba* ex gr. *E. controversa* Vachaard & Razgallah. 3) Equatorial section. Thin section 447. 5) Equatorial section. Thin section 449. 6) Equatorial section. Thin section 435. 7) Axial section. Thin section 451. 8) Oblique centred section. Thin section 438. 9) Axial section. Thin section 446.

Figs 10, 11 - *Endoteba* sp. Axial section. Mark the biconcave test shape. 10) Thin section 448. 11) Thin section 446.

Fig. 12 - *Trocholina*? *turris* Frentzen. Thin section 439.

Fig. 13 - *Aulotortus sinuosus* Weynschenk. Thin section 467.

Fig. 14 - *Triasina/Aulosina* sp. See possible internal pillars ("strengthenings" sensu Rigaud et al., 2013) transecting the chamber lumen (arrowead). Thin section 449.

Fig. 15 - *Planiinvoluta carinata* Leischner (white arrowhead) and possible *Decapoalina schaeferae* (Zaninetti, Altiner, Dager & Ducret) (grey arrowhead). Thin section 467.

Fig. 16 - *Galeanella tollmanni* (Kristan). Thin section 434.

Figs 17-18 - *Miliolipora tamarae* Gale, Rettori & Martini. Mark costae on the test surface (arrowhead) and quasi-quinqueloculine chamber arrangement. 17) Thin section 446. 18) Thin section 392.

PLATE 5

Foraminifera from the Slatnik Formation

Fig. 1 - *Miliolipora cuvillieri* Brönnimann & Zaninetti in Brönnimann, Zaninetti, Bozorgnia, Dashti & Moshtaghian. Thin section 465.

Fig. 2 - *Agathammina austroalpina* Kristan-Tollmann & Tollmann. Thin section 446.

Figs 3-4 - *Decapoalina schaeferae* (Zaninetti, Altiner, Dager & Ducret). 3) Thin section 438. 4) Thin section 430.

Fig. 5 - *Miliolechina stellata* Zaninetti, Ciarapica, Cirilli & Cadet. Thin section 446.

Fig. 6 - *Diplotremina subangulata* Kristan-Tollmann vel *Diplotremina placklesiana* Kristan-Tollmann. Thin section 411.

Fig. 7 - ? *Variostoma cochlea* Kristan-Tollmann. Thin section 464.

Figs 8-9 - *Variostoma coniforme* Kristan-Tollmann. 8) Thin section 448. 9) Thin section 395.

Figs 10-15 - Oberhauserellidae. 10) Thin section 388. 11) Thin section 395. 12) Thin section 397. 13) Thin section 398. 14-15) Thin section 411.

Figs 16-17 - Foraminifera. 16) Thin section 398. 17) Thin section 448.

Fig. 18 - *Pseudonodosaria* sp. Thin section 449.

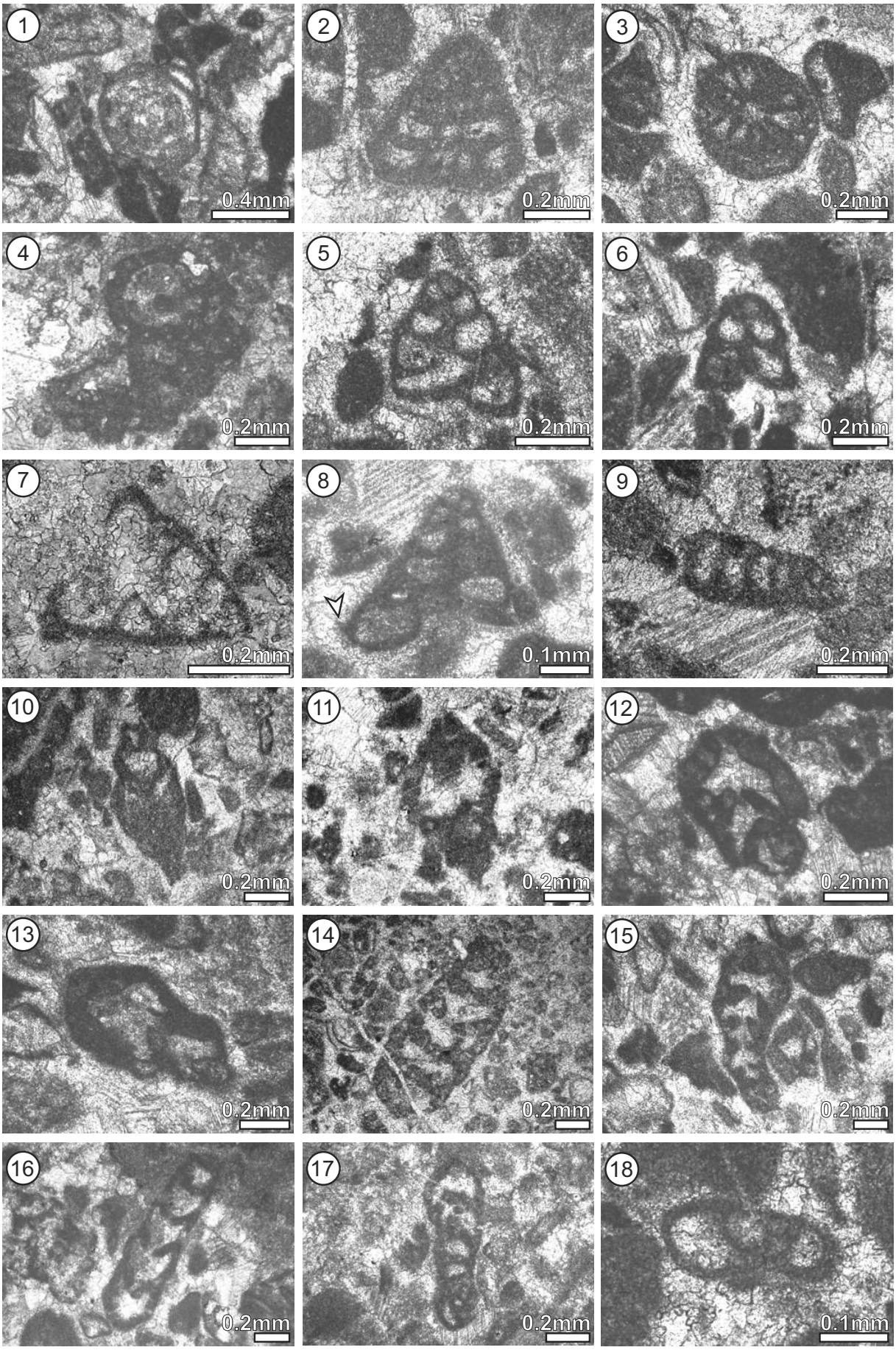
1
0.4mm
2
0.2mm
3
0.2mm
4
0.2mm
5
0.2mm
6
0.2mm
7
0.2mm
8
0.1mm
9
0.2mm
10
0.2mm
11
0.2mm
12
0.2mm
13
0.2mm
14
0.2mm
15
0.2mm
16
0.2mm
17
0.2mm
18
0.1mm

PLATE 3

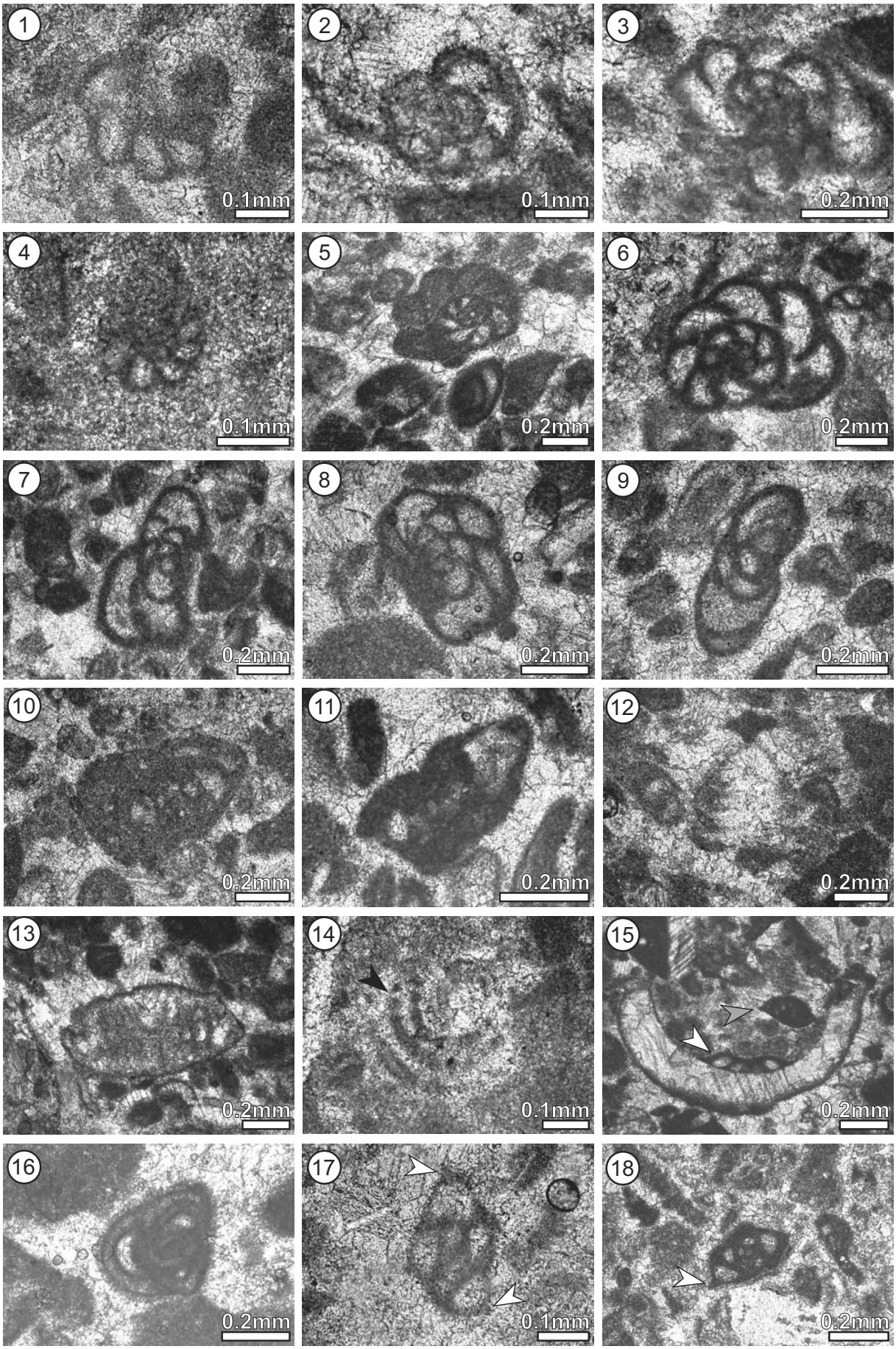
1
0.1mm
2
0.1mm
3
0.2mm
4
0.1mm
5
0.2mm
6
0.2mm
7
0.2mm
8
0.2mm
9
0.2mm
10
0.2mm
11
0.2mm
12
0.2mm
13
0.2mm
14
0.1mm
15
0.2mm
16
0.2mm
17
0.1mm
18
0.2mm

PLATE 4

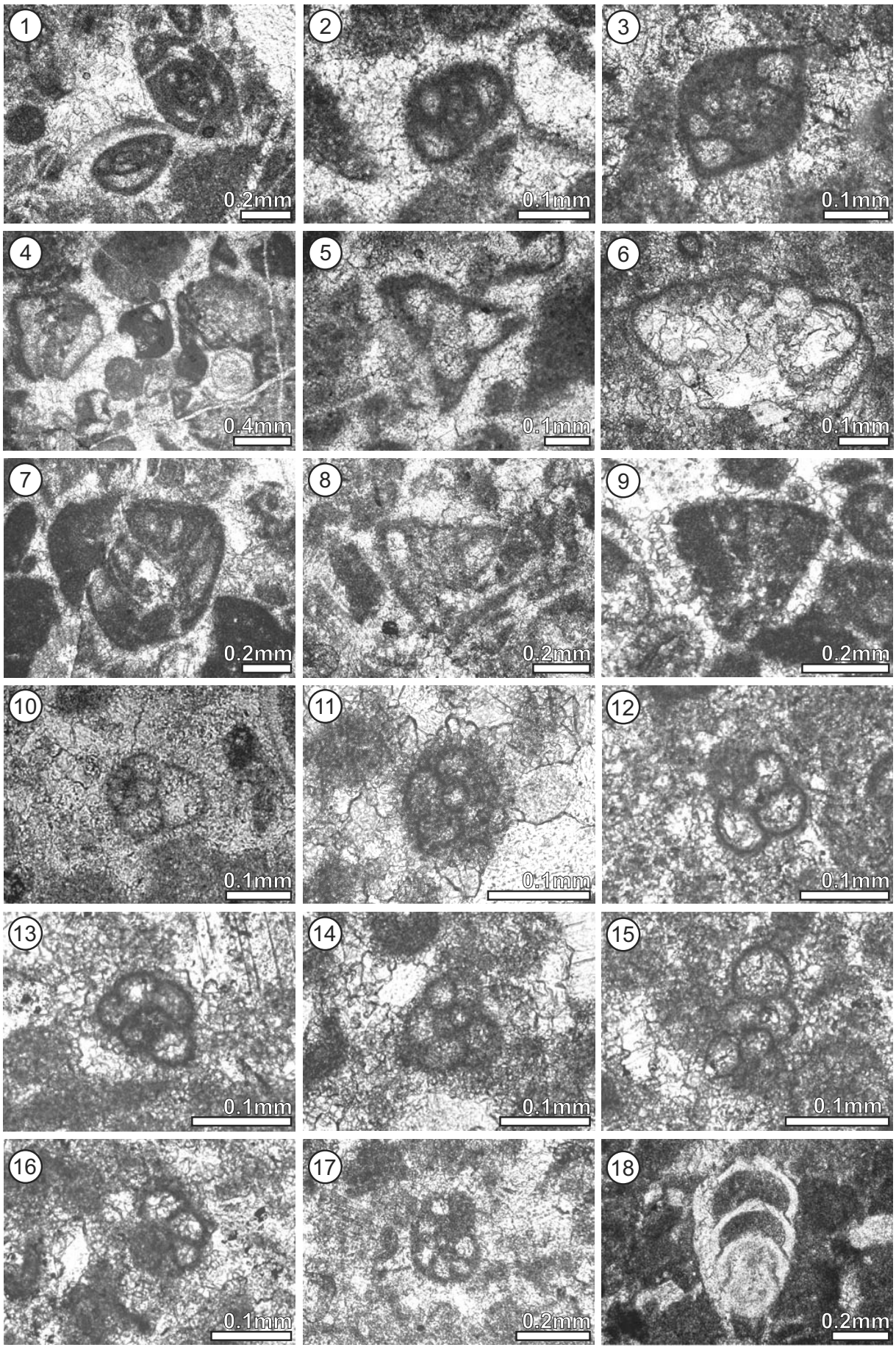
1
0.2mm
2
0.1mm
3
0.1mm
4
0.4mm
5
0.1mm
6
0.1mm
7
0.2mm
8
0.2mm
9
0.2mm
10
0.1mm
11
0.1mm
12
0.1mm
13
0.1mm
14
0.1mm
15
0.1mm
16
0.1mm
17
0.2mm
18
0.2mm

PLATE 5

al. 1998; Gawlick & Böhm 2000; Krystyn et al. 2009). However, as Maurer et al. (2003) noted, distal turbidites may be peloid-dominated solely due to grain sorting during transport. Boulders of silicified limestone with corals and cockades are interpreted as "Cipit blocks" s.l., i.e., gravity-displaced shallow-reef limestone blocks (see Wendt & Fürsich 1980; Biddle 1981; Wendt 1982; Russo et al. 1997; Trombetta 2011). These boulders together with several species of benthic foraminifera such as *Galeanella tollmanni*, *Decapoalina schaeferae*, *Kaeveria fluegeli*, and *Alpinophragmium perforatum* (see Gale 2012a with references), provide ample evidence for the existence of a coral-dominated reef on the rim of the carbonate platform.

The described MF types are randomly-distributed throughout the Slatnik Formation. However, it should be mentioned that sampling was targeted mostly at calciturbidites. Hemipelagic limestone predominates in the lower part of the Slatnik Formation. A notable feature of the lower part of the Slatnik Formation (Section A) is also the abundance of Oberhauserellidae (Pl. 5, figs 10-15). These are usually associated with the spreading of anoxic/disoxic waters during sea level rise (Hillebrandt 2012; Clémence & Hart 2013; Clémence & Hillebrandt 2013). Although first considered to be planktonic, they are now classified as opportunistic epibenthic grazers (Clémence & Hart 2013; Clémence & Hillebrandt 2013). Due to the lack of evidence for sluggish water conditions, and the failure to regard them as deep-water elements, we currently have no convincing explanation for the abundance of Oberhauserellidae in the lower part of Section A.

An upward-thickening trend is clearly visible in Sections B and C, where bedding becomes indistinct and very-thick bedded grainstone predominates from the 37th and 17th metres upward, respectively. This trend demonstrates the progradation of the Julian Platform towards the Slovenian Basin (see also Maurer et al. 2003). Due to limited visibility, it is impossible to distinguish clinoforms of the prograding wedge from the proximal Slatnik Formation, but the predominance of very-thick bedding and the lack of hemipelagites most likely mark the base of the prograding slope-and-rim of the Dachstein platform (see Figures 5, 6).

Norian progradation of the Julian Carbonate Platform

Extensive shallow-water carbonate deposition took place throughout the Neo-Tethys (e.g., Golonka 2007) during the Norian-Rhaetian. The Julian Platform (Fig. 7), situated at the western-most extension of the Neo-Tethys (see Haas et al. 1995), was characterised by the sedimentation of peritidal Dachstein Limestone (Ciarapica & Passeri 1990; Buser 1996; Ogorelec & Buser 1997; Sattler & Schlaf 1999). Margins of the Julian

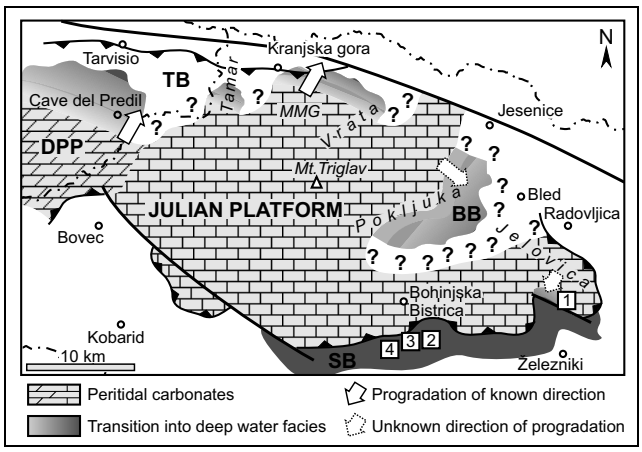

Fig. 7 - Present distribution of Late Norian facies units in the eastern Julian Alps (not palinspastically corrected). Full arrows indicate the recorded direction of platform margins towards adjacent basins (based on Gianolla et al. 2003; Celarc & Kolar-Jurkovšek 2008; Gianolla et al. 2010; Celarc et al. 2013). Dashed arrows indicate progradation with an unknown direction and rate (Buser et al. 1982; Jurkovšek 1987; Turnšek & Buser 1989; this paper). Note that the original relationships are strongly obscured by Paleogene to recent tectonic movements. For simplification, only major structural boundaries are drawn. The map is based on Placer (1999), Celarc and Kolar-Jurkovšek (2008), and Bavec et al. (2013).
Numbers in brackets indicate the positions of the following sections: 1- Jelovica sections (this study), 2- Mt. Slatnik section, 3- Mt. Kobla section, 4- Povdnar section (Rožič et al. 2013).
Abbreviations: BB- Bled Basin; DPP- Dolomia Principale Platform; MMG- Martuljek Mountain Group (Celarc & Kolar-Jukovšek 2008); SB- Slovenian Basin; TB- Tarvisio Basin (see Gianolla et al., 2010).

Platform and its transition to adjacent basins are rarely preserved due to the intense structural deformation related to collision of the northern margin of the Adria plate with the European margin (Kastelic et al. 2008).

Data from the eastern border of the Julian Alps, namely from the Pokljuka Plateau, suggest progradation of the platform (Buser et al. 1982; Jurkovšek 1987; Turnšek & Buser 1989); however, outcropping is poor, and the basin (Bled Basin sensu Cousin 1981; Goričan et al. 2012) into which the platform progrades is inadequately known. The platform margin is better defined towards the north, where it is more or less clear that progradation commenced at the end of the Carnian or in the lowermost Norian (Lieberman 1978; Ramovš 1985, 1986; Schlaf et al. 1997; Sattler & Schlaf 1999; De Zanche et al. 2000; Gianolla et al. 2003; Preto et al. 2005). From the Vrata Valley (Fig. 7) Schlaf et al. (1997) described a several hundred meters-thick succession of Tuvalian hemipelagic limestones and lower Norian slope deposits of the prograding platform followed by a short interval of bituminous micritic limestone. These deposits could reflect a short demise in progradation during the late Lacian (Gawlick & Böhm

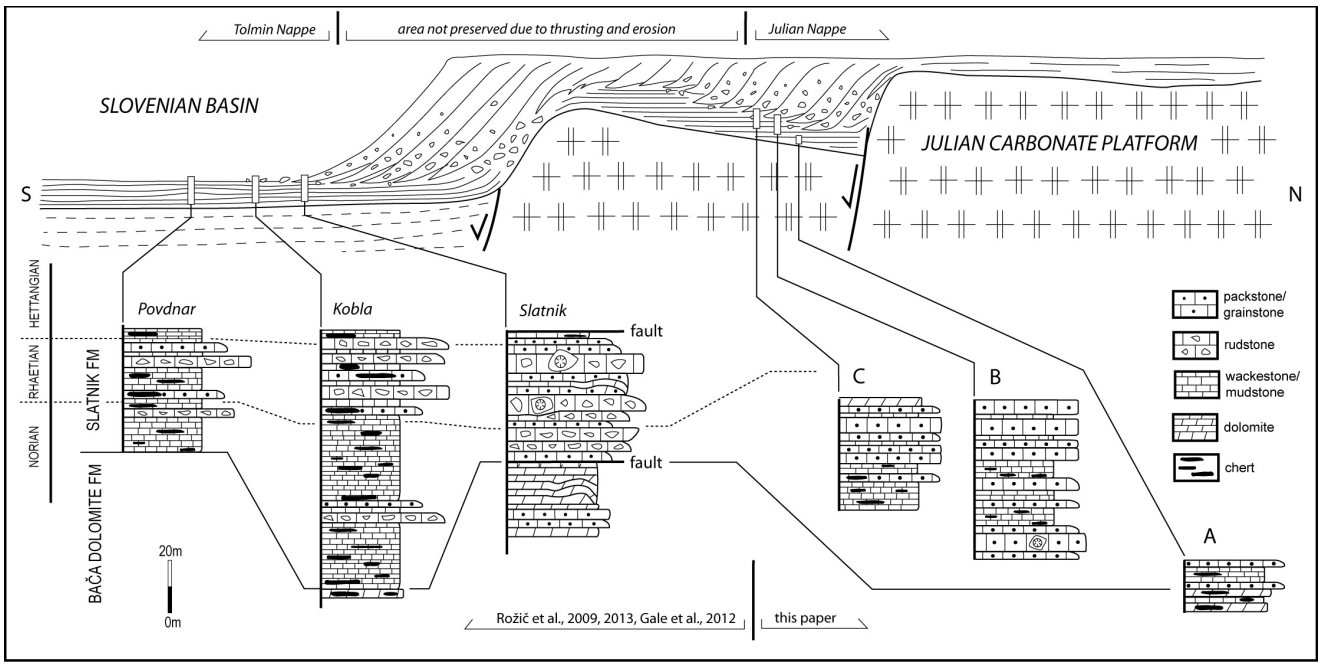

Fig. 8 - Authors view on the late Norian progradation of the Julian Platform towards the Slovenian Basin (based on Bosellini 1984). The hypothetically fault-controlled margin is chosen based on seismic-scale sections of the Dolomia Principale Platform (Carulli et al. 1998; Cozzi 2002). Povdnar, Mt. Kobla and Mt. Slatnik sections are redrawn from Rožič et al. (2009), Gale et al. (2012), and Rožič et al. (2013). The reef margin is left out of the illustration.

2000; Krystyn et al. 2009). Finally, clinoforms and platform-top carbonates follow.

Celarc & Kolar-Jurkovšek (2008) dated the transition from hemipelagic Martuljek platy limestone to prograding slope and reef margin facies of the Dachstein platform system in the Martuljek Mountain Group over a 5-km distance. The difference in age and the clinoform geometry point at SW-NE directed upper Tuvalian to lower Norian progradation of the platform at a rate of 1200 m/Myr (Celarc & Kolar-Jurkovšek 2008). This rate is in agreement with the progradation of the Dolomia Principale Platform over the hemipelagic Carnitza Formation, recorded in the Cave del Predil area (Lieberman 1978; De Zanche et al. 2000; Gianolla et al. 2003; Preto et al. 2005).

To the south, the platform carbonates are in contact with the strata of the Slovenian Basin along the prominent west-east-directed Krn thrust-fault (Buser 1987; Placer 1999, 2008). Dachstein-type reefs, located in the Bohinj Range at the southern border of the Julian Alps (Buser et al. 1982; Turnšek & Buser 1991; Turnšek 1997), suggest a reef-rimmed margin; however, information about the proximal slope itself is missing, and it is consequently impossible to recognise Norian-Rhaetian evolution of the (in the present orientation) southern platform margin. With the new data from the Jelovica plateau and the previously gathered information from the proximal Slovenian Basin (Rožič et al. 2009; Gale et al. 2012), we can now recognise similar pattern of platform evolution to the one recorded in the Northern Calcareous Alps (Krystyn et al. 2009; Gawlick & Böhm 2000).

The Norian-Rhaetian evolution of the adjacent Slovenian Basin recorded in sections on Mt. Slatnik, Mt. Kobla and the Povdnar section is schematically drawn in Figure 8. In all three sections, the lower, middle and part of the upper Norian correspond to the deposition of the Bača dolomite, while the deposition of the Slatnik Formation began in the late Norian and lasted until the end of Triassic (Rožič et al. 2009; Gale et al. 2012; Rožič et al. 2013).

In the Mt. Slatnik section, the lowermost part of the Slatnik Formation is missing due to a fault, and the lower part of the Slatnik Formation, dated as Sevatian in age (see Rožič et al. 2009; Gale et al. 2012; Rožič et al. 2013), thus spans only 15 m of the section. The incomplete dolomitisation of the upper 30 m of the Bača dolomite below allows the recognition of predominately thin-bedded wackestone and packstone with sedimentary textures attributable to the Bouma sequence. Up to 5.4 m, thick beds are an amalgamation of thin to medium-thick horizons of wackestone and packstone textures. In the uppermost part of the Bača dolomite, however, mudstone texture prevails in up to 40 cm thick beds. This part of the Bača dolomite presents part of a weakly pronounced late Norian progradation (Rožič et al. 2009). Crossing a fault, the dominance of mudstone and wackestone in medium-thick beds continues in the Slatnik Formation for another 8 m. Chert nodules and amalgamation are common. Subordinate coarser-

grained beds point at occasional sedimentation from turbidites. In the following 2 m thick part of the sequence coarse-grained packstone and fine-grained rudstone dominate. Below the Norian-Rhaetian boundary, set at the lowest occurrence of *Misikella posthernsteini* (Kozur & Mock), hemipelagics again become more prominent in a 3.5 m thick amalgamated succession, interspersed with calciturbidites. Above the Norian-Rhaetian boundary, a pronounced upward coarsening and thickening trend culminates approximately 10 m higher. Up to 3.5 m thick limestone-breccia beds with reef limestone boulders several metres in size have been set at the peak of the second prograding cycle by Rožič et al. (2009).

The Slatnik Formation is more complete in its type locality, the Mt. Kobla section, which is 2.3 km west of the Mt. Slatnik section. The Norian-Rhaetian boundary in this section is 73 m above the top of the Bača dolomite (Rožič et al. 2009; Gale et al. 2012; Rožič et al. 2013). With the exception of 6 m thick interval of graded or laminated packstone and convolutely laminated wackestone 28 m above the base of the Slatnik Formation, the Sevatian part of the Slatnik Formation predominantly consists of hemipelagic limestone, i.e., medium-thick mudstone with chert nodules. The mentioned coarser interval marks platform progradation and is equivalent to the progradation recorded in the upper part of the Bača dolomite in the Mt. Slatnik section. Calciturbidite intercalations become increasingly more frequent from the 68th metre of the Slatnik Formation upwards, i.e., 5 m below the Norian-Rhaetian boundary. This progradation, correlates to the second progradation in the Mt. Slatnik section and reaches its peak 5 m above the base of the Rhaetian (Rožič et al. 2009).

The Povdnar section is the westernmost of the three discussed sections from the Slovenian Basin. The Bača dolomite in the lower part of the section is marked by an at least 90 m thick succession of dolomitised debris and/or slump breccias, suggesting a strong tectonic influence in this part of the basin (Gale 2012a). Following a long covered interval and a few dolostone beds the upper Norian part of the Slatnik Formation spans for 20 m. Although three slump levels have been recorded in this part (Rožič et al. 2013), the hemipelagic sedimentation is uninterrupted by calciturbidite intercalations during the Sevatian, confirming a possible tectonic influence on sedimentation. A strong predominance of hemipelagic limestone with a few scattered packstone beds continues throughout the Rhaetian part of the formation. Thus, there is no sign of the first progradation phase, recorded in the Mt. Slatnik and Mt. Kobla sections, and only a very weak signal of the second, much stronger Rhaetian progradation is observed.

Of the three basinal sections, the Mt. Slatnik section presents deposition closest to the source area of calciturbidites, i.e., closest to the Julian Platform. In contrast, the Povdnar section has the most basinal character (Rožič et al. 2013). The Jelovica sections are located even further to the east and in the hanging wall of the South-Alpine thrust-fault. According to the geologic map (Fig. 2), the total thickness of the Slatnik Formation on the Jelovica plateau amounts to approximately 300 m in the Sevatian. Progradation of the platform, marked by thickening-upward calciturbidites and a general decline in hemipelagic sedimentation relative to gravity-flows, is evident here. While the late Norian progradation had little impact on sedimentation in the Slovenian Basin, platform wedge carbonates most likely closed the Jelovica part of the basin before the Rhaetian. According to Krystyn et al. (2009), and Gawlick & Böhm (2000), platform margin progradation accelerated in the early Rhaetian along the entire western border of the Neo-Tethys Ocean. This early Rhaetian progradation is strongly expressed in the Slovenian Basin as the main proximalisation phase of the Rhaetian.

Conclusions

The Jelovica plateau (W Slovenia) belongs structurally to the Krn (Julian) Nappe, a subunit of the eastern Southern Alps. This plateau's southern slopes record the transition between two late Triassic palaeogeographic units: the deep-water Slovenian Basin and the prograding Julian Carbonate Platform. The basinal strata are represented by the Norian Bača dolomite, while the Dachstein Limestone was deposited on the platform in a peritidal environment. The intermediate upper Norian Slatnik Formation records the transition from the basin to the prograding platform slope. Basinal sedimentation, represented by mudstone, radiolarian wackestone, and filament packstone, is more pronounced in the lower part of the Slatnik Formation. The proportion and thickness of calciturbidites, i.e., peloidal-bioclastic wackestone, graded bioclastic-peloidal packstone and grainstone, and lithoclastic-bioclastic-intraclastic grainstone/rudstone, increases moving upwards, suggesting progradation of the adjacent carbonate platform. Cipit boulders and some benthic foraminifera from calciturbidites point at the reef-rimed platform margin. The late Norian platform progradation is consistent with the progradation of platforms in the western Neo-Tethys Ocean during the Norian highstand (Reijmer et al. 1991; Gianolla et al. 1998; Gawlick & Böhm 2000; Krystyn et al. 2009; Haas et al. 2010b). Progradation is much more poorly expressed in the deeper parts of the Slovenian Basin (Rožič et al. 2009; Gale et al. 2012;

Rožič et al. 2013). The marginal part of the basin, preserved on the Jelovica plateau, was completely filled by prograding platform wedge most likely by the beginning of the Rhaetian.

Acknowledgments. We are thankful to the Slovenian Research Agency for providing the financial support for this research (program number P1-0011). We extend our gratitude to reviewers for constructive comments. The technical staff of the Geological Survey of Slovenia is acknowledged for the preparation of samples.

REFERENCES

Baccelle L. & Bosellini A. (1965) - Diagrammi per la stima visiva della composizione percentuale nelle rocce sedimentarie. *Univ. studi Ferrara, Annali. Nuova ser. Sez. IX: Sci. Geol. Paleontol.*: 59-62.

Bavec M., Car M., Stopar R., Jamšek P. & Gosar A. (2012) - Geophysical evidence of recent activity oft he Idrija fault, Kanomljy, NW Slovenia. *RMZ – Materials and Geoenvironment*, 59: 247-256.

Bavec M., Novak M. & Poljak M. (2013) - Geological map of Slovenia 1: 1 million. Geološki zavod Slovenije, Ljubljana.

Berra F. & Cirilli S. (1997) - Palaeoenvironmental interpretation of the Late Triassic Fraele Formation (Ortles Nappe, Austroalpine Domain, Lombardy). *Riv. It. Paleont. Strat.*, 103: 53-70.

Berra F., Jadoul F. & Anelli A. (2010) - Environmental control on the end of the Dolomia Principale/Hauptdolomit depositional system in the central Alps: Coupling sea-level and climate changes. *Palaeogeogr., Palaeoclimatol., Palaeoecol.*, 290: 138-150.

Biddle K.T. (1981) - The basinal cipit boulders: indicators of Middle to Upper Triassic buildup margins, Dolomite Alps, Italy. *Riv. It. Paleont. Strat.*, 86: 779-794.

Borsato A., Frisia S. & Sartorio D. (1994) - Late Triassic – Early Liassic stratigraphic and diagenetic evolution of the margin between the Trento Platform and the Lombardy Basin in the Brenta Dolomites (Italy). *Studi Trentini Sci. Natur. Acta Geol.*, 69 (1992): 5-35.

Bosellini A. (1984) - Progradation geometries of carbonate platforms: examples from the Triassic of the Dolomites, northern Italy. *Sedimentology*, 31: 1-24.

Bosellini A., Gianolla P. & Stefani M. (2003) - Geology of the Dolomites. *Episodes*, 26: 181-185.

Brenchley P.J. & Harper D.A.T. (1998) - Palaeoecology: ecosystems, environments and evolution. V. of 402 pp. Chapman & Hall, The Alden Press, Oxford.

Brenčič M. (2003) - Hidrogeološke razmere v napajalnem zaledju izvirov Kroparice pod Jelovico. *Geologija*, 46: 281-306.

Budkovič T. (1978) - Stratigrafija Bohinjske doline. *Geologija*, 21: 239-244.

Buser S. (1986) - Explanatory book, Sheet Tolmin and Videm (Udine) L 33-64, L 33-63. Basic geological map of SFRJ 1: 100.000. V. of 103 pp. Zvezni Geološki Zavod, Beograd.

Buser S. (1987) - Basic geological map SFRJ 1:100.000, sheet Tolmin & Videm (Udine), L33-64. Zvezni geološki zavod, Beograd.

Buser S. (1989) - Development of the Dinaric and the Julian carbonate platforms and of the intermediate Slovenian Basin. *Mem. Soc. Geol. It.*, 40: 313-320.

Buser S. (1996) - Geology of Western Slovenia and its paleogeographic evolution. In: Drobne K., Goričan Š. & Kotnik B. (Eds) - International workshop Postojna '96: The role of impact processes and biological evolution of planet Earth: 111-123, Ljubljana.

Buser S. & Debeljak I. (1993) - Lower Jurassic beds with bivalves in south Slovenia. *Geologija*, 37-38: 23-62.

Buser S., Ramovš A. & Turnšek D. (1982) - Triassic reefs in Slovenia. *Facies*, 6: 15-24.

Buser S., Kolar-Jurkovšek T. & Jurkovšek B. (2008) - The Slovenian Basin during the Triassic in the light of conodont data. *Boll. Soc. Geol. It.*, 127: 257-263.

Carulli G.B., Cozzi A., Salvador G.L., Ponton M. & Podda F. (1998) - Evidence of synsedimentary tectonic activity during the Norian-Lias (Carnian Prealps, Northern Italy). *Boll. Soc. Geol. It.*, 53: 403-415.

Castellarin A., Vai GB. & Cantelli L. (2006) - The Alpine evolution of the Southern Alps around the Giudicarie faults: A Late Cretaceous to Early Eocene transfer zone. *Tectonophysics,* 414: 203-223.

Celarc B. & Kolar-Jurkovšek T. (2008) - The Carnian-Norian basin-platform system of the Martuljek Mountain Group (Julian Alps, Slovenia): progradation of the Dachstein carbonate platform. *Geol. Carpathica,* 59: 211-224.

Celarc B., Gale L. & Kolar-Jurkovšek T. (2013) - Stratigrafski razvoj zgornjetriasnih plasti doline Tamar (severne Julijske Alpe) in primerjava s sosednjimi globljemorskimi razvoji. In: Rožič B. (Ed) - 21st meeting of Slovenian geologists. *Geol. zbornik*, 22: 21-25.

Ciarapica G. & Passeri L. (1990) - The Dachstein Limestone of the Mt. Canin (Julian Alps) and its paleogeographic meaning. *Boll. Soc. Geol. It.*, 109: 239-247.

Clémence M.-E. & Hart M.B. (2013) - Proliferation of Oberhauserellidae during the recovery following the Late Triassic extinction: paleoecological implications. *J. Paleont.*, 87: 1004-1015.

Clémence M.-E. & Hillebrandt A.v. (2013) - Oberhauserellidae (benthic foraminifera) outbursts during the environmental perturbations at the Triassic-Jurassic boundary: palaeoecological implications. In: Georgescu M.D. (Ed.) - Foraminifera: aspects of classification, stratigraphy, ecology and evolution. Marine Biology, Earth Sciences in the 21st century. Nova Science Publishers: 1-26.

Cousin M. (1981) - Les rapports Alpes-Dinarides; Les confins de l'Italie et de Yougoslavie. Vol. I. *Soc. Géol. Nord*, 5: 1-521.

Cozzi A. (2002) - Facies patterns of a tectonically-controlled Upper Triassic platform-slope carbonate depositional system (Carnian Prealps, Northeastern Italy). *Facies,* 47: 151-178.

Cozzi A. & Podda F. (1998) - A platform to basin transition in the Dolomia Principale of the M. Pramaggiore area, Carnia Prealps, northern Italy. *Mem. Soc. Geol. It.*, 53: 387-402.

De Zanche V., Gianolla P. & Roghi G. (2000) - Carnian stratigraphy in the Raibl/Cave del Predil area (Julian Alps, Italy). *Eclogae Geol. Helv.*, 93: 331-347.

Doglioni C. & Bosellini A. (1987) - Eoalpine and mesoalpine tectonics in the Southern Alps. *Geol. Rund.*, 76: 735-754.

Dunham R.J. (1962) - Classification of carbonate rocks according to depositional texture. In: Han W.E. (Ed.) - Classification of carbonate rocks, A symposium. *Amer. Ass. Petrol. Geol. Mem.*: 108-121.

Flügel E. (2004) - Microfacies of carbonate rocks: Analysis, interpretation and application. V. of 976 pp. Springer-Verlag, Berlin Heidelberg.

Frisia S. (1994) - Mechanisms of complete dolomitization in a carbonate shelf: comparison between the Norian Dolomia Principale (Italy) and the Holocene of Abu Dhabi Sabkha. In: Purser B.H., Tucker M.E. & Zenger D.H. (Eds) - Dolomites: a volume in honour of Dolomieu. *Int. Ass. Sedimentol. Spec. Publ.*, 21: 55-74.

Gale L. (2010) - Microfacies analysis of the Upper Triassic (Norian) "Bača Dolomite": early evolution of the western Slovenian Basin (eastern Southern Alps, western Slovenia). *Geol. Carpathica,* 61: 293-308.

Gale L. (2012a) - Rhaetian foraminiferal assemblage from the Dachstein Limestone of Mt. Begunjščica (Košuta Unit, eastern Southern Alps). *Geologija,* 55: 17-44.

Gale L. (2012b) - Biostratigrafija in sedimentologija norijsko-retijskih plasti zahodnega Slovenskega bazena, Južne Alpe, Slovenija [PhD Thesis]. V. of 268 pp. University of Ljubljana, Ljubljana.

Gale L., Kolar-Jurkovšek T., Šmuc A. & Rožič B. (2012) - Integrated Rhaetian foraminiferal and conodont biostratigraphy from the Slovenian Basin, eastern Southern Alps. *Swiss J. Geosci.*, 105: 435-462.

Galli M.T., Jadoul F., Bernasconi S.M., Cirilli S. & Weissert H. (2007) - Stratigraphy and palaeoenvironmental analysis of the Triassic-Jurassic transition in the western Southern Alps (Northern Italy). *Palaeogeogr., Palaeoclimatol., Palaeoecol.*, 244: 52-70.

Gawlick H.-J. & Böhm F. (2000) - Sequence and isotope stratigraphy of Late Triassic distal periplatform limestones from the Northern Calcareus Alps (Kälberstein Quarry, Berchtesgaden Hallstatt Zone). *Int. J. Earth Sci. (Geol. Rundsch.),* 89: 108-129.

Gianolla P., De Zanche V. & Mietto P. (1998) - Triassic sequence stratigraphy in the Southern Alps (Northern Italy): definition of sequences and basin evolution. In: De Graciansky P.C., Hardenbol J., Jacquin T. & Vail P.R. (Eds) - Mesozoic and Cenozoc Sequence Stratigraphy of European Basins: *SEPM Spec. Publ.*, 60: 719-746.

Gianolla P., De Zanche V. & Roghi G. (2003) - An Upper Tuvalian (Triassic) platform-basin system in the Julian Alps: the start-up of the Dolomia Principale (Southern Alps, Italy). *Facies,* 49: 125-150.

Gianolla P., Mietto P., Rigo M., Roghi G. & De Zanche V. (2010) - Carnian-Norian paleogeography in the eastern Southern Alps. In: Di Stefano P. & Balini M. (Eds) - New Developments on Triassic Integrated Stratigraphy. Museo Geologico "G. G. Gemmellaro": 21, Palermo.

Golonka J. (2004) - Plate tectonic evolution of the southern margin of Eurasia in the Mesozoic and Cenozoic. *Tectonophysics*, 381: 235-273.

Golonka J. (2007) - Late Triassic and Early Jurassic palaeogeography of the world. *Palaeogeogr., Palaeoclimatol., Palaeoecol.*, 244: 297-307.

Goričan Š., Košir A., Rožič B., Šmuc A., Gale L., Kukoć D., Celarc B., Črne A.E., Kolar-Jurkovšek T., Placer L. & Skaberne D. (2012) - Mesozoic deep-water basins of the eastern Southern Alps (NW Slovenia). *J. Alp. Geol.*, 54: 101-143.

Grad K. & Ferjančič L. (1974) - Basic geological map SFRJ 1:100.000, sheet Kranj, L 33-65. Zvezni geološki zavod, Beograd.

Grad K. & Ferjančič L. (1976) - Explanatory book, Sheet Kranj L 33-65. Basic geological map of SFRJ 1: 100.000. V. of 70 pp. Zvezni Geološki Zavod, Beograd.

Grafenauer S. (1980) - Petrologija triadnih magmatskih kamnin na Slovenskem. V. of 220 pp. Slovenska akademija znanosti in umetnosti, Razred za prirodoslovne vede, Ljubljana.

Grgasović T. (2003) - Revizija rodova *Physoporella* Steinmann i *Oligoporella* Pia (Dasycladales) [PhD Thesis]. V. of 484 pp. Sveučilište u Zagrebu, Zagreb.

Haas J. & Budai T. (1999) - Triassic sequence stratigraphy of the Transdanubian Range (Hungary). *Geol. Carpathica,* 50: 459-475.

Haas J. & Tardy-Filácz E. (2004) - Facies changes in the Triassic-Jurassic boundary interval in an intraplatform basin succession at Csővár (Transdanubian Range, Hungary). *Sed. Geol.*, 168: 19-48.

Haas J., Kovács S., Krystyn L. & Lein R. (1995) - Significance of Late Permian-Triassic facies zones in terrane reconstructions in the Alpine-North Pannonian domain. *Tectonophysics*, 242: 19-40.

Haas J., Piros O., Budai T., Görög Á, Mandl G. & Lobitzer H. (2010a) - Transition between the massive reef-backreef and cyclic lagoon facies of the Dachstein Limestone in the southern part of the Dachstein Plateau, Northern Calcareous Alps, Upper Austria and Styria. *Abh. Geol. B.-A.*, 65: 35-56.

Haas J., Budai T., Piros O., Szeitz P., Görög Á. (2010b) - Late Triassic platform, slope and basin deposits in the Pilis Hills, Transdanubian Range, Hungary. *Central European Geology,* 53: 233–260.

Hillebrandt A.v. (2012) - Are the Late Triassic to Early Jurassic aragonitic Oberhauserellidae (Robertinina) the

ancestors of planktonic Foraminifera. *N. Jb. Geol. Paläont. Abh*., 266: 199-215.

Iannace A., Boni M., Climaco A. & Zamparelli V. (1994) - The platform-to-basin transition in the Upper Triassic of "Verbicario unit" (Calabria, Southern Italy). *C. R. Acad. Sci. Paris*, 318: 197-204.

Iannace A., Capuano M. & Galluccio L. (2011) - "Dolomites and dolomites" in Mesozoic platform carbonates of the Southern Apennines: Geometric distribution, petrography and geochemistry. *Palaeogeogr., Palaeoclimatol., Palaeoecol*., 310: 324-339.

Jadoul F., Galli M.T., Muttoni G., Rigo M. & Cirilli S. (2007) - The late Norian-Hettangian stratigraphic and paleogeographic evolution of the Bergamasc Alps. In: Geoitalia 2007, Pre-Congress Field Trip Guide Book – FW02: 1-33, Rimini.

Jurkovšek B. (1987) - Explanatory book, Sheet Beljak & Ponteba L 33-51, L 33-52. Basic geological map of SFRJ 1: 100.000. V. of 58 pp. Zvezni Geološki Zavod, Beograd.

Kastelic V. & Carafa M.M.C. (2012) - Fault slip rates for the active External Dinarides thrust-and-fold belt. *Tectonics*, 31: TC3019.

Kastelic V., Vrabec M., Cunningham D. & Gosar A. (2008) - Neo-Alpine structural evolution and present-day tectonic activity of the eastern Southern Alps: The case of the Ravne Fault, NW Slovenia. *J. Struct. Geol.,* 30: 963-975.

Kidwell S.M. & Bosence D.W.J. (1991) - Taphonomy and time-averaging of marine shelly faunas. In: Allison P.A. & Briggs D.E.G. (Eds) - Taphonomy: Releasing the Data Locked in the Fossil Record. *Topics in Geobiology*, 9: 115-209. Plenum Press, New York.

Kolar-Jurkovšek T. (1991) - Mikrofavna srednjega in zgornjega triasa Slovenije in njen biostratigrafski pomen. *Geologija,* 33: 21-170.

Kossmat F. (1914) - Geologie des Wocheiner Tunnels und der Südlichen Anschlusslinie. *Denkschr. Kais. Akad. Wiss. Math.-Nat. Klasse*, 82: 6-142.

Kristan-Tollmann E. (1964) - Die Foraminiferen aus den Rhätischen Zlambachmergeln der Fischerwiese bei Aussee im Salzkammergut. *Jb. Geol. B.-A*., spec. issue 10: 1-189.

Krystyn L., Richoz S., Gallet Y., Bouquerel H., Kürschner W.M. & Spötl C. (2007) - Updated bio- and magnetostratigraphy from Steinbergkogel (Austria), candidate GSSP for the base of the Rhaetian stage. *Albertiana*, 36: 164-172.

Krystyn L., Mandl G.W. & Schauer M. (2009) - Growth and termination of the Upper Triassic platform margin of the Dachstein area (Northern Calcareous Alps, Austria). *Austrian J. Earth Sci*., 102: 23-33.

Lieberman H.M. (1978) - Carnitza Formation. *Mitt. Ges. Geol. Bergbaustud. Österr*., 25: 35-60.

Mancinelli A., Chiocchini M., Chiocchini R.A. & Romano A. (2005) - Biostratigraphy of Upper Triassic-Lower Jurassic carbonate platform sediments of the central-southern Apennines (Italy). *Riv. It. Paleont. Strat.*, 111: 271-283.

Mandl G.W. (2000) - The Alpine sector of the Tethyan shelf – Examples of Triassic to Jurassic sedimentation and deformation from the Northern Calcareous Alps. *Mitt. Österr. Geol. Gess*., 92: 61-77.

Martini R., Zaninetti L., Lathuilliere B., Cirilli S., Cornée J.-J. & Villeneuve M. (2004) - Upper Triassic carbonate deposits of Seram (Indonesia): palaeogeographic and geodynamic implications. *Palaeogeogr., Palaeoclimatol., Palaeoecol.*, 206: 75-102.

Maurer F., Reijmer J.J.G. & Schlager W. (2003) - Quantification of input and compositional variations of calciturbidites in a Middle Triassic basinal succession (Seceda, Dolomites, Southern Alps). *Int. J. Earth Sci. (Geol. Rundsch.)*, 92: 593-609.

Mazza M., Rigo M. & Gullo M. (2012) - Taxonomy and biostratigraphic record of the Upper Triassic conodonts of the Pizzo Mondello section (western Sicily, Italy), GSSP candidate for the base of the Norian. In: Proceedings of the Palermo Workshop "New Developments on Triassic Integrated Stratigraphy", Palermo, September 12-16, 2010. *Riv. It. Paleont. Strat.*, 118: 85-130.

Meister P., McKenzie J.A., Bernasconi S.M. & Brack P. (2013) - Dolomite formation in the shallow seas of the Alpine Triassic. *Sedimentology*, 60: 270-291.

Ogorelec B. & Buser S. (1997) - Dachstein limestone from Krn in Julian Alps (Slovenia). *Geologija*, 39: 133-157.

Ogorelec B. & Rothe P. (1993) - Mikrofazies, Diagenese und Geochemie des Dachsteinkalkes und Hauptdolomits in Süd-West-Slowenien. *Geologija*, 35: 81-181.

Oravecz-Scheffer A. (1987) – Triassic foraminifers of the Transdanubian central range. *Geol. Hung. Ser. Paleont.,* 50: 1-331.

Pálfy J., Demény A., Haas J., Carter E.S., Görög Á., Halász D., Oravecz-Scheffer A., Hetényi M., Márton E., Orchard M.J., Ozsvárt P., Vető I. & Zajzon N. (2007) - Triassic-Jurassic boundary events inferred from integrated stratigraphy of the Csővár section, Hungary. *Palaeogeogr., Palaeoclimatol., Palaeoecol*., 244: 11-33.

Placer L. (1999) - Contribution to the macrotectonic subdivision of the border region between Southern Alps and External Dinarides. *Geologija*, 41: 223-255.

Placer L. (2008) - Principles of the tectonic subdivision of Slovenia. *Geologija*, 51: 205-217.

Placer L. & Čar J. (1998) - Structure of Mt. Blegoš between the Inner and the Outer Dinarides. *Geologija*, 40: 305-323.

Pleničar M. (2000) - Geološka zgradba širšega Radovljiškega prostora. In: Dežman J. (Ed) - Med Jelovico in Karavankami, Radovljiški zbornik 2000: 9-33, Radovljica.

Pleničar, M., Ogorelec, B. & Novak, M. (2009). The Geology of Slovenia. V. of 612 pp. Geological Survey of Slovenia, Ljubljana.

Preto N., Roghi G. & Gianolla P. (2005) - Carnian stratigraphy of the Dogne area (Julian Alps, northern Italy): tessera of a complex palaeogeography. *Boll. Soc. Geol. Ital*., 124: 269-279.

Ramovš A. (1985) - Geološke raziskave severnih Julijskih Alp in njihov biostratigrafski razvoj. *Jeklo in ljudje, jeseniški zbornik*, 5: 391-428.

Ramovš A. (1986) - Paläontologisch bewiesene Karn/Nor-Grenze in den Julischen Alpen. *Newslett. Strat*., 16: 133-138.

Ramovš A. (2001) - Lipoldovo geološko raziskovanje in njegove rokopisne karte slovenskega ozemlja. *Geologija*, 44: 7-14

Reijmer J.J.G., Tenkate W.G.H.Z., Sprenger A. & Schlager W. (1991) - Calciturbidite composition related to exposure and flooding of a carbonate platform (Triassic, Eastern Alps). *Sedimentology*, 38: 1059-1074.

Reijmer J.J.G., Palmieri P. & Groen R. (2012) - Compositional variations in calciturbidites and calcidebrites in response to sea-level fluctuations (Exuma Sound, Bahamas). *Facies*, 58: 493-507.

Rigaud S., Martini R. & Rettori R. (2013) - A new genus of Norian involutinid foraminifers: its morphological, biostratigraphic, and evolutionary significance. *Acta Palaeont. Pol*., 58: 391-405.

Rožič B. (2006) - Stratigrafija, sedimentologija in geokemija jurskih plasti zahodnega dela Slovenskega jarka [PhD Thesis]. V. of 149 pp. Univerza v Ljubljani, Ljubljana.

Rožič B. (2008) - Upper Triassic and Lower Jurassic limestones from Mt Kobla in the northern Tolmin Basin: tectonically repeated or continuous succession? *RMZ – Materials and Geoenvironment*, 55: 345-362.

Rožič B. & Šmuc A. (2011) - Gravity-flow deposits in the Toarcian Perbla Formation (Slovenian Basin, NW Slovenia). *Riv. It. Paleont. Strat*., 117: 283-294.

Rožič B., Kolar-Jurkovšek T. & Šmuc A. (2009) - Late Triassic sedimentary evolution of Slovenian Basin (eastern Southern Alps): description and correlation of the Slatnik Formation. *Facies,* 55: 137-155.

Rožič B., Gale L. & Kolar-Jurkovšek T. (2013) - Extent of the Late Norian and Rhaetian Slatnik Formation in the Tolmin Thrust, eastern Southern Alps. *Geologija,* 56: 175-186.

Russo F., Neri C., Mastandrea A. & Baracca A. (1997) - The mud mound nature of the Cassian platform margins of the Dolomites. A case history: the cipit boulders from Punta Grohmann (Sasso Piatto Massif, northern Italy). *Facies*, 36: 25-36.

Sattler U. & Schlaf J. (1999) - Sedimentologie und Mikrofazies des gebankten Dachstein-kalkes der Julischen Alpen Sloweniens (Obertrias). *Mitt. Ges. Geol. Bergbaustud. Österr.*, 42: 109-118.

Schlaf J., Lein R. & Krystyn L. (1997) - Sequence stratigraphy of Upper Triassic carbonate platform margins in the Julian Alps (Slovenia) – an example for tectonic control on the development of systems tracts. *Gaea Heidelberg.,* 3: 303-304.

Schlager W., Reijmer J.J.G. & Droxler A. (1994) - Highstand shedding of carbonate platforms. *J. Sed. Res*., B64/3: 270-281.

Skaberne D., Goričan Š. & Čar J. (2003) - Kamnine in fosili (radiolariji) iz kamnoloma Kamna Gorica. *Vigenjc*, 3: 85-100.

Šmuc A. (2005) - Jurassic and Cretaceous stratigraphy and sedimentary evolution of the Julian Alps, NW Slovenia. V. of 98 pp. ZRC Publishing, Ljubljana.

Trombetta G.L. (2011) - Facies analysis, geometry and architecture of a Carnian carbonate platform: the Settsass/Richthofen reef system (Dolomites, Southern Alps, northern Italy). *Geo. Alp*, 8: 56-75.

Tucker M. (2001) - Sedimentary petrology (3rd edition). V. of 262 pp. Blackwell Science, Osney Nead, Oxford.

Tucker M. (2003) - Sedimentary rocks in the field (3rd edition). V. of 234 pp. John Wiley & Sons Ltd, Chippenham.

Turnšek D. (1997) - Mesozoic corals of Slovenia. V. of 470 pp. ZRC Publishing, Ljubljana.

Turnšek D. & Buser S. (1989) - The Camian reef complex on the Pokljuka (NW Yugoslavia). *Razprave IV. razreda SAZU*, 30: 75-127.

Turnšek D. & Buser S. (1991) - Norian-Rhaetian coral reef buildups in Bohinj and Rdeči Rob in southern Julian Alps (Slovenia). *Razprave IV. razreda SAZU*, 32: 215-257.

Velić I. (2007) - Stratigraphy and palaeobiology of Mesozoic benthic foraminifera of the Karst Dinarides (SE Europe). *Geologia Croatica*, 60: 1-113.

Vetters H. (1933) - Geologische Karte von Radmannsdorf (Radovljica), 1:75.000. Zusammengestellt nach Originalaufnahmen von Teller, V. F. (1910-1912), Kossmat, F. (1913), Haertel, F. (Julische Alpen, 1920) & Ampferer, O. (Saveterrassen, 1910). *Geol. R.-A*., Wien.

Vrabec M. & Fodor L. (2006) - Late Cenozoic tectonics of Slovenia: structural styles at the Northeastern corner of the Adriatic microplate. In: Pinter N., Grenerczy G., Weber J., Stein S. & Medek D. (Eds) - The Adria microplate: GPS geodesy, tectonics and hazards. *NATO Sci. Ser., IV, Earth Envir. Sci.*, 61: 151-168.

Vrabec M., Pavlovčič Prešeren P. & Stopar B. (2006) - GPS study (1996-2002) of active deformation along the Periadriatic fault system in northeastern Slovenia: tectonic model. *Geol. Carpathica*, 57: 57-65.

Vrabec M., Šmuc A., Pleničar M. & Buser S. (2009) - Geological evolution of Slovenia – an overview. In: Pleničar M., Ogorelec B. & Novak M. (Eds) - The geology of Slovenia. Geološki zavod Slovenije: 23-40 Ljubljana.

Watts K.F. (1987) - Triassic carbonate submarine fans along the Arabian platform margin, Sumeini Group, Oman. *Sedimentology*, 34: 43-71.

Wendt J. (1982) - The Cassian patch reefs (Lower Carnian, Southern Alps). *Facies*, 6: 185-202.

Wendt J. & Fürsich F.T. (1980) - Facies analysis and palaeogeography oft he Cassian Formation, Triassic, Southern Alps. *Riv. It. Paleont. Strat.*, 85: 1003-1028.

Zupan N. (1990) - Geomorfološke značilnosti Jelovice. In: Gavrilović D., Petrović D. & Manojlović P. (Eds) - Četvrti skup geomorfologa Jugoslavije: Pirot, 20-23 juna 1989. Geografski fakultet PMF: 87-93, Beograd.

Zupan-Hajna N. (1995) - Geološka podoba Lipniške doline. In: Štekar-Vidic V. (Ed) - Kroparski zbornik: ob 100-letnici Plamena (1894-1994). Tovarna vijakov Plamen & Občina Radovljica: 30-38, Kropa & Radovljica.